Genome-wide identification of GH9 gene family and the assessment of its role during fruit abscission zone formation in Vaccinium ashei

Weiwei Zheng (zhengww@zafu.edu.cn)
Zhejiang A and F University https://orcid.org/0000-0002-3927-774X
Yingying Wang
Zhejiang A and F University
Yue Xu
Zhejiang A and F University
Fangfang Liao
Zhejiang A and F University
Ting Li
Zhejiang A and F University
Xiaolong Li
Zhejiang A and F University
Boping Wu
Zhejiang A and F University
Seung-Beom Hong
University of Houston-Clear Lake
Kai Xu
Zhejiang A and F University
Yunxiang Zang
Zhejiang A and F University

Research Article

Keywords: Vaccinium ashei, Genome-wide analysis, Expression pattern, Glycosyl hydrolase

Posted Date: April 17th, 2023

DOI: https://doi.org/10.21203/rs.3.rs-2783726/v1

Version of Record: A version of this preprint was published at Plant Cell Reports on July 20th, 2023. See the published version at https://doi.org/10.1007/s00299-023-03049-y.

Abstract

Glycosyl hydrolase family 9 (GH9) cellulases play a crucial role in both cellulose synthesis and hydrolysis during plant growth and development. Despite this importance, there is currently no study on the involvement of GH9-encoding genes, specifically VaGH9s, in abscission zone formation of rabbiteye blueberries (Vaccinium ashei). In this study, we identified a total of 61 VaGH9s in the genome, which can be classified into three subclasses based on conserved motifs and domains, gene structures, and phylogenetic analyses. Our synteny analysis revealed that VaGH9s are more closely related to the GH9s of Populus L. than to those of Arabidopsis, Vitis vinifera, and Citrus sinensis. In-silico structural analysis predicted that most of VaGH9s are hydrophilic, and localized in cell membrane and/or cell wall, and the variable sets of cis-acting regulatory elements and functional diversity with four categories of stress response, hormone regulation, growth and development, and transcription factor-related elements are present in the promoter sequence of VaGH9s genes. Transcriptomic analysis showed that there were 22 differentially expressed VaGH9s in fruit abscission zone tissue at the veraison stage, and the expression of VaGH9B2 and VaGH9C10 was continuously increased during fruit maturation, which were in parallel with the increasing levels of cellulase activity and oxidative stress indicators, suggesting that they are involved in the separation stage of fruit abscission in Vaccinium ashei. Our work identified 22 VaGH9s potentially involved in different stages of fruit abscission and would aid further investigation into the molecular regulation of abscission in rabbiteye blueberries fruit.

Key message

The genomic location and stage-specific expression pattern of GH9 genes reveal their critical roles during fruit abscission zone formation in *Vaccinium ashei*.

Introduction

Abscission is a natural process by which organs are shed through cell separation at specific sites called abscission zones (AZs). AZs are narrow bands of functionally specialized cell layers that respond to a range of cues such as developmental, hormonal, and environmental signals. Abscission occurs via at least four stages: (i) pre-formation stage in which cells are differentiated to form AZs at the future sites of organ detachment (Estornell et al. 2013; Ma et al. 2021); (ii) induction stage in which AZs cells become competent in response to abscission signals and activated to begin elongation (Patharkar and Walker 2018); (iii) separation stage in which cell wall degradation enzymes are produced to weaken cell adhesion (Roberts et al. 2002); and (iv) protective layer formation stage in which protective compounds are secreted to cover the wound surface of the separated cells and shield from desiccation (Estornell et al. 2013). The regulation of the rate and degree of abscission is heavily influenced by the delicate balance and interplay of phytohormones. Ethylene and abscisic acid are known to promote abscission, while gibberellins and auxins inhibit it (Botton and Ruperti 2019; Colle et al. 2019). Interestingly, jasmonic acid has been found to have a distinctive effect on different plants; it stimulated fruit abscission in grapes, while it delayed ethylene-induced petal abscission in roses (Fidelibus et al. 2022; Priya et al. 2022;

Sawicki et al. 2015). The abscission process involves multiple cell wall remodeling enzymes including cellulase, an endo-β-1,4-glucanase that is widely found in both plants and cellulolytic microorganisms (Kalaitzis et al. 1999). Glycoside hydrolase family 9 (GH9) genes (http://www.cazy.org/), which primarily code for endo-β-1,4-glucanases, have been identified in various plant species, including, but not limited to, *Arabidopsis thaliana*, *Oryza sativa*, *Populus* L., and these genes were shown to be associated with diverse aspects of plant growth and development (Cantarel et al. 2009; Dheilly et al. 2016; Xie et al. 2013; Yu et al. 2014). The crystal structure showed a high degree of conservation in both secondary and tertiary structures, as well as catalytic and carbohydrate binding amino acid residues in certain species (Gray et al. 2018). Plant-derived GH9 enzymes typically consist of 441 to 694 amino acid residues, with a calculated and observed molecular mass ranging from 42 to 70 kDa. Their structures feature 12 alpha helices that are comprised of six inner and outer alpha helices forming an α/α barrel shape with six parallel alpha helices (Du et al. 2015; Yu et al. 2014). The GH9 family proteins can be divided into three distinct structural subclasses, with GH9A having a single NH_2-terminal transmembrane helix and a catalytic domain, GH9B having a signal peptide and a catalytic domain, and GH9C having a COOH-terminal carbohydrate binding module (CBM) in addition to a signal peptide and catalytic domain (Del et al. 2012; Urbanowicz et al. 2007).

The *GH9* genes in higher plants have evolved specific functions such as cell division and elongation, cytokinesis, anther dehiscence, pollen tube growth, organ abscission, and fruit ripening (Campillo et al. 2012; Szyjanowicz et al. 2004; Yu et al. 2014; Zhou et al. 2006). Although many GH9 proteins have been functionally studied in multiple plants, including *Arabidopsis thaliana* (Zuo et al. 2000), *Oryza sativa L.* (Xie et al. 2013), *Populus* L. (Yu et al. 2014), *Triticum* (Szyjanowicz et al. 2004), and *Fragaria ananassa* (Luo et al. 2022), their roles in cellulose synthesis and assembly remain poorly understood. All 74 *Triticum GH9* genes (*TaGH9s*) identified encode hydrophilic proteins, and subcellular localization predictions revealed that *TaGH9* proteins act in the cytoplasm, Golgi complex, mitochondria, endoplasmic reticulum, and nucleus (Szyjanowicz et al. 2004). Previous studies have found that individual genes in *GH9* family are involved in the regulation of cellulose content and cellulase activity. For example, *OsGH9B1*, *3*, and *16*, are associated with cellulase activity according to the catalytic domain analysis (Xie et al. 2013). Cellulase activity was promoted by the increased expression of *CEL1* and *CEL2* genes during fruit development in *Fragaria ananassa* (Mercado et al. 2010). However, mutation of *OsGLU1* in *Oryza sativa* resulted in the decreased cellulose content, suggesting that *OsGLU1* affects the cellulose biosynthesis of *Oryza sativa* (Campillo et al. 2012). The *KOR1* in *GH9* family, which is located primarily in the plasma membrane, plays an important role in cellulose metabolism of both primary and secondary cell walls in *Arabidopsis* and *Populus L.* (Yu et al. 2014; Zuo et al. 2000).

Rabbiteye blueberry (*Vaccinium ashei*) has been increasingly cultivated in China due to their good adaption to high temperatures and acidic (pH 4.0–5.3) soil conditions (He et al. 2009). This fruit is known for its potent benefits for consumers (Davidson et al. 2018; Mercado et al. 2010) and has unique fruit development and ripening, with all berries in the same inflorescence taking at least one month to fully abscise from the main plant body. In recent years, abscission has become a focus of research due to its

significant negative impact on crop yield and fruit quality when it occurs prematurely. Additionally, in some crops like cotton and citrus, accelerated abscission at a proper time is necessary to facilitate improved harvest and labor savings. As a result, many abscission studies have been carried out in fruit crops including, but not limited to, citrus (Sabbione et al. 2019), apple (Arseneault et al. 2016), litchi (Wang et al. 2019), sweet cherry (Qiu et al. 2020), blueberry (Vashisth et al. 2013; Vashisth et al. 2015) orange (Merelo et al. 2017) and tomato (Brummell et al. 1999). It has been pointed out that fruit abscission mainly results from the disassembly of cell layers at fruit AZs which is driven by cell wall-degrading enzymatic activities (Liu et al. 2019; Wang et al. 2019). As the fruit matures, there is an increasing tendency of cellulase activity in fruit AZs (Li et al. 2019a; Merelo et al. 2017). In recent years, 25 *GH9* genes in *Arabidopsis*, 24 *GH9* genes in rice, 22 *GH9* genes in barley, 29 *GH9* genes in corn, 25 *GH9* genes in poplar, and 7 *GH9* genes in wheat have been identified (Buchanan et al. 2012; Du et al. 2015; Xie et al. 2013; Yu et al. 2014;). To date, there is no systematic study of the *GH9* gene family in *Vaccinium ashei* despite the crucial role of cellulase in abscission. The recent completion of *Vaccinium ashei* genomic release allowed us to study the *GH9* gene family at the genome level (Colle et al. 2019; Main et al. 2018). In this article, we investigated the gene structure, chromosomal location, conserved motifs and domains of *Vaccinium ashei GH9* genes (*VaGH9s*), conducted phylogenetic and syntenic analyses between *GH9* genes in *Arabidopsis thaliana*, *Populus L.*, *Vitis vinifera*, *Citrus sinensis*, and *Vaccinium ashei*, and analyzed the expression of *VaGH9s* in abscission zone during fruit development in the presence and absence of ethephon and gibberellins. This study presents the first report on genome-wide *VaGH9s* profile analysis and the differential expression of *VaGH9s* in fruit AZs during fruit development of *Vaccinium ashei*.

Materials And Methods

Plant material and in vitro treatments

Ten-year-old rabbiteye blueberry (*Vaccinium ashei*) cv. ‘Brightwell’, grown in Zhejiang A&F University was used in this study. During the veraison stage, the trees were treated with either gibberellin (200 mg/L), ethephon (500 mg/L), or water (served as control). The berries at relatively consistent maturity and without mechanical damage were picked at seven-day intervals. The abscission zone (AZ) tissues at fruit-pedicel junction were immediately isolated and brought to the Key Laboratory of Quality and Safety Control for Subtropical Fruit and Vegetable, Ministry of Agriculture and Rural Affairs for the analysis of microstructure and the measurement of cellulase activity, reactive oxygen species (ROS), malondialdehyde (MDA), and relative conductivity. The AZ tissues from the berries at the veraison stage were isolated 0 h and 24 h after gibberellin (200 mg/L) or ethephon (500 mg/L) treatment and frozen into liquid nitrogen for transcriptome analysis.

Collection and identification of VaGH9 genes in Vaccinium ashei

The reference genome and gene model annotation files were retrieved from the blueberry genome website (https://www.vaccinium.org/crop/blueberry) (Colle et al. 2019). To obtain all the *GH9* sequences in

Vaccinium ashei, we performed BLASTn homology searches against the *Vaccinium ashei* genome datasets using the full-length coding sequences of *Arabidopsis GH9s* as queries. Candidate *GH9* genes were selected if it was satisfied with $E < 10^{-10}$. Subsequently, the deduced amino acid sequences of candidate genes were analyzed to detect glycosyl hydrolase family 9 (IPR001701) domains from the InterPro protein signature database (https://www.ebi.ac.uk/interpro/) (Mistry et al. 2021), and the related and aligned sequences were retrieved from the *Vaccinium ashei* genome datasets using HMMER3.0 software (https://www.ebi.ac.uk/Tools/hmmer/) (Potter et al. 2018). We provisionally named the candidate sequences *VaGH9A1* to *VaGH9C12* following the standardized nomenclature of the *GH9* family in *Arabidopsis* to distinguish them (Urbanowicz et al. 2007) (Table S1).

Analysis of physico-chemical properties of VaGH9s

ProtParam tool (https://web.expasy.org/protparam/) was used to analyze the amino acids, molecular weights, grand average of hydropathy (GRAVY) and theoretical isoelectric points of *Vaccinium ashei GH9* family members. CELLO v.2.5 /CELLO2GO (https://mybiosoftware.com/ cello-v-2-5-subcellular-localization-predictor.html) was used to predict the subcellular localization of *Vaccinium ashei GH9* family members (Chou et al. 2010).

Phylogenetic Analysis

AtGH9 protein sequences of *Arabidopsis* were obtained from the TAIR database (https://www.arabidopsis.org/). *Populus L.* PtrGH9, *Vitis vinifera* VitGH9, and *Citrus sinensis* CsGH9 protein sequences were obtained from NCBI (https://www.ncbi.nlm.nih.gov). Multiple alignments of *Arabidopsis*, *Populus L.*, *Vitis vinifera*, *Citrus sinensis*, and *Vaccinium ashei* GH9 protein sequences were performed using ClustalW of MEGA X (Kumar et al. 2018). Phylogenetic trees were constructed with MEGA X using the neighbor-joining (NJ), minimal evolution (ME), and maximum parsimony (MP) methods, and bootstrap values were based on 1000 replicates.

Exon/intron Structure, Conserved Motifs, Domains And Promoter Analysis

The exon-intron arrangement was visualized with the gene structure display server (GSDS) using both genomic DNA sequences and the corresponding coding sequences (http://gsds. gao-lab. org/) (Hu et al. 2015). Conserved motifs of GH9 proteins were analyzed using the MEME Version 4.11.4 program (http://meme.nbcr.net/meme/tools/meme).The following parameters was used: motif width set to 6–200 and the maximum number of motifs set to 10 (Bailey et al. 2009). The MEME motifs were annotated using the InterPro database (https://www.ebi.ac.uk/interpro/), and the conserved domain database was used to predict the conserved domains of the *GH9* family members of *Vaccinium ashei*. The 2.0-kb DNA sequences upstream of ATG were retrieved from the genome database to predict the *cis*-acting regulatory

elements using PlantCARE (http://bioinformatics.psb.ugent.be/webtools/plantcare/html/) (Lescot et al. 2002).

Chromosomal Location And Gene Synteny Analysis

The positions of *GH9*-encoding genes on the chromosomes of *Vaccinium ashei* and aforementioned plants were obtained from the NCBI (https://www.ncbi.nlm.nih.gov). The synteny analysis among members of *Vaccinium ashei GH9* family and between *Vaccinium ashei* and *Arabidopsis*, *Populus L.*, *Vitis vinifera*, and *Citrus sinensis* were performed using MCScanX and TBtools (Chen et al. 2020; Wang et al. 2012).

Rna Isolation And Transcriptome Sequencing Analysis

The total RNAs from AZs samples were extracted using #RC401 test kit according to the manufacturer's instructions (Vazyme Biotech Co., Ltd), and RNA quality was verified with an Agilent 2100 Bioanalyzer. Transcriptome libraries were constructed following the standard Illumina RNA-seq protocol (Illumina, Inc., San Diego, CA, catalog no. RS-100-0801). RNA and DNA libraries were sequenced using a 150-bp paired-end Illumina sequencing, with libraries having inserts of 350 bp. For RNA-seq, the raw reads were filtered using fastp (v 0.12.2) with default parameter to eliminate those reads with poly-N, adapter, and low qualities (Chen et al. 2018). The filtered high-quality reads were mapped on the V_corymbosum_genome_v1.0 genome (Kulkarni et al. 2020) using Hisat2 (v 2.1.0) with parameters (–dta, -x) followed by gene annotation in GTF format (Trapnell et al. 2012). Genes with a minimum FPKM (Fragments Per Kilobase of transcript per Million mapped reads) value > 1 in any sample were defined as being expressed. Differentially expressed genes were identified based on $P = 0.05$ and a two-fold difference cut-off using DEseq2 (Liu et al. 2021a).The heat map analysis of gene expression was performed with TBtools software (Wang et al. 2012).

Qrt-pcr Analysis

Total RNA was extracted from the AZs tissues at four phenological stages of young fruitlet (S1), swelling (S2), veraison (S3), and full maturity (S4). The qRT-PCR expression analysis of selected genes was conducted using the primers designed by Primer 3 (Table S4). The *POLYUBIQUITIN 3* (*UBQ3b*) gene was used as an internal control since it was found to be one of the most stably expressed genes across multiple organs in rabbiteye blueberry (Vashisth et al. 2011). The qRT-PCR with SYBR Premix Ex Taq II (TaKaRa) was repeated at least three times, and the data were analyzed using the $2^{-(\Delta\Delta Ct)}$ method (Livak et al. 2001).

Observation Of Azs Structure

The AZs tissues were fixed in FAA (50% ethanol, 5% glacial acetic acid, 10% formalin, and 35% water by volume) for a minimum of 24 h and stored at 4°C. They were then dehydrated with ethanol, embedded in molten paraplast, and sectioned into 10 μm thick ribbons using a Microm HM 355S microtome (ThermoFisher, Waltham, MA, USA). The slides were viewed using an Olympus BX60 microscope, and images were captured by an Olympus DP70 camera.

Cellulase Activity, And Other Characteristics Assays

Cellulase activity was measured according to the carboxymethyl cellulose (CMC) method (Ghose et al. 2013). The production rate of O_2^- was measured by monitoring the formation of nitrite (NO_2^-) from hydroxylamine, and the absorbance was measured at 530 nm (Jambunathan et al. 2010). The determination of H_2O_2 content was based on the absorbance of the titanium-peroxide complex at 415 nm as described by Qian et al. (Qian et al. 2013). Relative conductivity and malondialdehyde (MDA) were measured as previously described (Li et al. 2016).

Results

Identification and in **s** ilico **analysis of** VaGH9 **genes in** Vaccinium ashei

It has been documented that *GH9* is involved in cell wall modification by controlling cellulose synthesis and hydrolysis, thereby playing the significant roles in various processes of plant growth and development (Bhandari et al. 2006; Campillo et al. 2012; Shani et al. 2006; Szyjanowicz et al. 2004; Zhou et al. 2006; Zuo et al. 2000). Thus, we implemented *in silico* analysis of *GH9* gene family of *Vaccinium ashei* in terms of gene structures, physicochemical properties, structural motifs, chromosomal locations, and phylogenetic relationship before *VaGH9s* were functionally addressed in the AZs formation. A total of 61 *VaGH9s* were genome-widely identified using HMMER3.0 method, and the redundant forms of the same gene were removed simultaneously (see Material and Method). *GH9* family was divided into three distinct structural subclasses (A, B, and C) and were named *VaGH9A1* to *VaGH9C12* according to the standardized nomenclature of the GH9 family in *Arabidopsis* (Urbanowicz et al. 2007) (Table S1).

We analyzed and compared the physicochemical characteristics of VaGH9s proteins, such as amino acids (aa) composition, molecular weight (MW), isoelectric point (pI), hydrophobicity, and subcellular location (Table S1). Analysis of deduced protein sequence revealed that all 61 candidate VaGH9s proteins comprised the Glyco_hydro_9 domains (PF00759) with similar physicochemical properties. The predicted proteins encoded by VaGH9s had a range of length from 156 to 1368 aa, with a molecular mass ranging from 17.5 kDa (for VaGH9C9) to 152.6 kDa (for VaGH9A1). There were 35 acidic and 26 basic proteins, with the pI varying between 4.68 (for VaGH9C8) and 10.16 (for VaGH9B36). Most of the VaGH9 proteins were hydrophilic, with a grand average of hydropathicity (GRAVY) score less than 0. However, VaGH9A1 was a hydrophobic protein with a GRAVY score of 0.088. *In silico* analysis for subcellular localization predicted that 33 VaGH9s reside in both the cell membrane and cell wall, with 23

VaGH9s in the cell membrane and 5 VaGH9s in the cell wall. Taken together, the physicochemical properties of the proteins encoded by members of *VaGH9* gene family appear to be distinct and divergent.

Phylogenetic Analysis And Classification Of Vagh9 Genes

To explore the evolutionary relationships between VaGH9s and GH9 proteins from other plants, we constructed a neighbor-joining phylogenetic tree using MEGA 7.0 (Kumar et al. 2016). The analysis revealed that VaGH9 proteins formed three Clades (A, B, and C) and clustered together with GH9 enzymes from other plant species (Fig. 1). Clade B, the largest subclass, consisted of 38 VaGH9 proteins (designated as VaGH9 B1-38); Clade C had 12 VaGH9 proteins (designated as VaGH9 C1-12); and Clade A, the smallest subclass, included 11 VaGH9 proteins (designated as VaGH9 A1-11).

It is notable that certain *VaGH9s* belong to the same clade as GH9s with known function in the phylogenetic tree. For example, *VaGHA1-3* were grouped with *AtGH9A1* and *PtrKOR*, both of which are membrane-bound endo-1,4-ß-D-glucanases involved in the cellulose biosynthesis of both primary and secondary cell walls, and they play a role in cell wall loosening during root hair formation and growth (Boraston et al. 2004; Shani et al. 2006). The *VaGH9s* family may have undergone evolutionary diversification similar to that of its counterparts in four other plant species. The degree of sequence similarities between GH9 proteins in *Vaccinium ashei* and *Populus L.* (13.04%) were found to be higher compared to the similarity between *Vaccinium ashei* and *Arabidopsis* (12.83%), *Vitis vinifera* (12.24%), and *Citrus sinensis* (12.78%). This suggests that GH9 proteins in *Vaccinium ashei* are more closely related to *Populus L* than to the other plants.

Gene structure analysis of VaGH9s **in** Vaccinium ashei

The *VaGH9* gene family was divided into three subgroups according to the phylogenetic tree constructed from the amino acid sequences (Fig. 2A). To examine the organization of exons/introns, we compared the genomic and cDNA sequences of all *VaGH9* members. The coding sequences of the entire *VaGH9* family were interrupted by introns, with the number of exons ranging from 2 to 17 (Fig. 2B). Comparison of intron-exon structure of *VaGH9A* showed that most genes in Clade A have 5–7 exons, while *VaGH9A1* contains 17 exons. Additionally, *VaGH9A8-11* have one more exon than *VaGH9A2-4*. Clade B, represented by 38 members of *VaGH9B* group, is the largest and most diverse subclass in the *VaGH9* family, and the number of introns in this group ranges from one to thirteen, with lengths varying from 52 to 9,798 bp within the transcriptional regions (Fig. 2B). The majority of *VaGH9s* in Clade B have 5–8 exons, but there are some exceptions: *VaGH9B4* and *VaGH9B30* both contain 11 exons, while *VaGH9B3*, *VaGH9B5*, *VaGH9B6*, *VaGH9B32*, and *VaGH9B33* all have 14 exons. The number of introns ranges from one (*VaGH9B36*) to sixteen (*VaGH9A1*). *VaGH9C1-4* has one large intron (2965–3332 bp) and some small introns. Meanwhile, *VaGH9C5-7* have seven small introns with length varying from 89 to 906 bp (Fig. 2B). Therefore, individual exons and introns vary considerably in number and size within and between the clades. In particular, 29 *VaGH9s* in clades A, B, and C have both 5’ and 3’ UTR, and the remaining *VaGH9s*

lack either 5'-UTR or 3-UTR, suggesting that expression of *VaGH9* genes is subject to at least three different post-transcriptional regulation processes. These findings imply that *VaGH9s* within the same clade having similar gene structures characterized by comparable numbers and phases of introns have evolved to the gene family expansion with limited functional diversification of the proteins, but with distinct regulation, stability, and localization of mRNA.

Conserved motifs and domains analyses of VaGH9s

The conserved motifs and domains were analyzed to further understand the functions of *VaGH9s*. In this study, we identified ten motifs and seven domains (Fig. 3A), and their annotations are provided in Table S2. Many closely related members in the phylogenetic tree were found to exhibit common motifs at the same alignment and position, suggesting that members of *GH9* that are clustered in the same subgroup may have similar biological functions. A total of 44 VaGH9 proteins were found to have the motifs 1–10 in order, except for VaGH9A1-7, VaGH9A11, VaGH9B11-13, VaGH9B35-36, and VaGH9C8-12. The VaGH9A1-7 proteins within clade A lack only motif 5, while all members of clade C contain motif 5. All VaGH9B proteins in clade B have motifs 9–10, except for VaGH9B35 and VaGH9B36, which only have motifs 1 and 6. Particularly, VaGH9C12 carries motif 5 only. In general, the protein sequences of the members of the VaGH9 family are relatively conserved, and all the VaGH9 proteins possess Glyco_hydro_9 domain at comparable positions where all ten motifs are located (Fig. 3B). It is notable that VaGH9B30 protein has both PME and PMEI domains that are involved in pectin degradation (Wormit and Usadel 2018), whereas VaGH9B7 had PME domain only. The CBM49 domain that promotes the interaction of the enzyme with target carbohydrates (Boraston et al. 2004) is located at the C-terminal region of VaGH9C5-8 proteins. Unlike most of other hydrophilic VaGH9 proteins, the hydrophobic VaGH9A1 has a distinctive feature with three discrete domains known as Ferric_reduct, FAD-binding 8, and NAD-binding 6. Thus, each clade has its own VaGH9s harboring unique domains that are absent in other VaGH9s within the same clade. However, the overall compositions of motifs and domains, as well as the lengths of VaGH9s except for 14 proteins (A1, B3-6, B30, B32-33, B35-36, C9-12) are very similar. This suggests the presence of limited functional diversity within a high degree of functional redundancy in the paralogous genes in the same clades.

Cis **-acting regulatory elements in the promoter regions of** VaGH9s

Genes with similar expression patterns are likely to have shared transcriptional regulation and common *trans*-acting binding sites. The *cis*-acting regulatory DNA sequences play a critical role in transcriptional control of temporal and spatial gene expression in response to developmental and environmental cues (Schmitz et al. 2022). In addition, expression divergence resulting from distinct *cis*-acting elements of the members of gene family may enhance understanding of the biological significance of different mechanisms of gene duplication. Thus, to further understand the regulatory mode of *VaGH9* gene expression, we analyzed the promoter region of each *VaGH9* for *cis*-acting regulatory elements (CAREs) by scanning a 2-kb upstream genomic sequence (Fig. 4A). We identified four categories of CAREs: stress response, plant growth and development, hormone regulation and transcription factor (Fig. 4B). Fifteen

types of *cis*-elements were found to be associated with stress response, such as myeloblastosis (MYB) and myelocytometosis (MYC) elements, anaerobic induction element (ARE), low-temperature responsiveness (LTR), defense and stress responsiveness (TC-rich repeats) and wound-responsive element (WUN-motif) among others. The MYB is the most prevalent element in this category, accounting for 23.78%, followed by MYC at 20.48%. Notably, all of 61 *VaGH9s* possess MYB in common. In the category of plant growth and development, sixteen types of *cis*-elements were detected, including activating sequence-1 (as-1), meristem expression element (CAT-box), zein metabolism regulation element (O2-site), circadian control element, endosperm expression element (GCN4_motif) among others. The as-1 was the most common element in this category, accounting for 26.95%, followed by AAGAA-motif at19.04%. In the hormone-responsive category, 16 types of *cis*-element were found, including ABRE related to ABA (abscisic acid) responsiveness (39.1%), CGTCA-motif and TGACG-motif responsive to jasmonic acid methyl ester (MeJA) (29.3%), four types of *cis*-elements related to auxin responsiveness (AuxRR-core, AuxRE, TGA-element, and TGA-box) (10.2%), P-box and GARE-motif related to gibberellin (GA) responsiveness (7.9%), TCA-element, TCA, SARE responsive to salicylic acid (SA)(7.8%), and ERE responsive to ethylene (ETH) (5.7%). In the transcription factor category, four types of *cis*-elements were determined: MYB binding site responsive to drought inducibility (MBS) (54.35%), MYB binding site involved in light responsiveness (MRE) (8.71%), and MYB binding site involved in flavonoids biosynthetic genes regulation (MBS1) (6.51%). In addition, CCAAT-box was found to be the binding site of transcription factor MYBHv1, representing 30.43% of the transcription factor category (Fig. 4C).

Chromosomal localization and synteny analysis of VaGH9s

Gene duplication is a key mechanism that contributes to functional diversity. To identify the duplication events in *VaGH9* genes, a collinearity analysis was performed using MCScanX software (Fig. 5). Among 61 *VaGH9s*, 50 were unevenly distributed in 34 *Vaccinium ashei* scaffold chromosomes, and the exact locations of the remaining eleven were not determined (Fig. 5). Twenty one chromosomes harbor one *VaGH9*, while two *VaGH9s* are separately distributed on each of ten chromosomes and three *VaGH9s* in each of three chromosomes 12, 27 and 28. A total of 86 pairs of fragment duplication were found in 48 *VaGH9* genes, with the highest number of duplications observed in chromosome 12 and no duplicated gene pairs in chromosomes 9 and 36. *VaGH9B30* on chromosome 15 was found to have collinearity to *VaGH9B7*, *VaGH9B25*, *VaGH9B26*, *VaGH9B27*, *VaGH9B28*, *VaGH9B29*, and *VaGH9B31*. This expansion of *VaGH9* gene family across the chromosomes is indicative of the occurrence of whole genome duplication (WGD) resulting in a balanced gene drive (Freeling et al. 2009). In addition, the number of gene pairs between *Vaccinium ashei* and other species was not correlated with the size of their genomes. The evolutionary rates and selective pressure of the *VaGH9* gene family was estimated by calculating non-synonymous/synonymous substitution ratio (Ka/Ks) (Table S5). The results showed that the ratio is less than 1, with values ranging from 0 to 0.92, suggesting that *VaGH9s* in the *Vaccinium ashei* genome primarily evolved under the influence of a purifying selection process that removes deleterious mutations from a population (Del et al. 2021).

The syntenic relationships between *VaGH9* and *GH9* genes from four other plant species (*Arabidopsis*, *Populus L.*, *Vitis vinifera*, and *Citrus sinensis*) were analyzed using MEGAX (Fig. 6). The genome size of the species was ordered as follows: *Vitis vinifera* (469.7Mb) (Jaillon et al. 2007), *Populus L.* (419.5Mb) (Tuskan et al. 2006), *Citrus sinensis* (317.2 Mb) (Wang et al. 2014), and *Arabidopsis thaliana* (115.6 Mb) (Korbinian et al. 2011). The results showed that *VaGH9s* have 64 orthologous pairs with *Populus L.*, followed by 45 with *Arabidopsis* (n = 49), 42 with *Vitis vinifera* (n = 43), and 41 with *Citrus sinensis* (n = 43) (Table S3). This indicated that *Vaccinium ashei* is more closely related to *Populus* L. than the other three plants, which is consistent with the degree of relationship based on sequence similarity.

Transcriptomic profiles and differential expression of VaGH9s in fruit AZs at the version stage of Vaccinium ashei in response to ethylene and gibberellins

To identify the differentially expressed genes (DEGs) associated with AZs formation, we analyzed RNA-seq data from fruit AZs at the version stage in the absence (Ctrl) and presence of ethylene and gibberellins with three biological replicates. DEGs were determined by pairwise comparison of the expression data. As compared with Ctrl, ethephon treatment significantly up-regulated 2958 DEGs and down-regulated 2732 DEGs, while gibberellin treatment significantly up-regulated 121 DEGs and down-regulated 277 DEGs. The Venn diagram showed that the number of genes identified in Ctrl, ethephon, and gibberellins were 398, 5690, and 2623, respectively (Fig. 7). Among them, 107, 4833, and 1838 DEGs were specifically expressed in Ctrl, ethephon, and gibberellin, respectively. To identify the function of sets of genes impacted, we conducted a GO-term enrichment analysis of DEGs in ethephon and gibberellins relative to Ctrl. DEGs genes were enriched in cell wall degradation, secondary metabolism, and growth-promoting hormone synthesis.

In total, 22 DEGs (marked with stars in Fig. 1) were identified in fruit AZs tissues. To identify group of DEGs that are co-regulated, their expression profiles were displayed as a heatmap. As shown in Fig. 8A, they can be categorized into five groups based on their expression patterns. The first group of *VaGH9s* (*B11, B12, B13, C12*) showed significant down-regulation after 24 h without treatment (C0 versus C24C), and they were not considerably affected by ethephon treatment (C24C versus C24E). However, their expression levels were significantly increased after gibberellin treatment (C24C versus C24G), although they remained much lower than those in control group (C0 versus C24G). The second group of *VaGH9s* (*B9, B10*) was strongly up-regulated by gibberellin (C24C versus C24G) and down-regulated by ethephon (C24C versus C24E). The third group of *VGH9s* (*B14, B15, B16, B17, C5, C6, C7, C8, C10, C11*) was strongly up-regulated by ethephon and either weakly up-regulated or unaffected by gibberellin. The fourth group of *VaGH9s* (*A1, A2, A3, B1, B2*) was fairly up-regulated by both ethephon and gibberellin. Finally, *VaGH9B24* expression was not significantly affected by ethephon and gibberellin treatment but markedly reduced after 24 h.

VaGH9s expression profiles in AZs at four phenological stages

Eight *VaGH9s* (*A1*, *A2*, *B2*, *B9*, *B12*, *B14*, *C7*, *C10*) were chosen to investigate their qRT-PCR expression profiles in AZs tissues at four fruit developmental stages (Fig. 8B). As shown in Fig. 8C, the expression

levels of *VaGH9A1* and *VaGH9C7* continually decreased, whereas those of *VaGH9B2* and *VaGH9C10* continually increased as the fruit development advanced. Interestingly, expression of *VaGH9A2*, *VaGH9B12*, and *VaGH9B14* was culminated at the S2 stage (swelling stage), after which their expression gradually declined during fruit maturation. The expression of the *VaGH9B9* also reached its peak at the S2 stage, after which their expression decreased in the veraison (S3) stage and increased during fruit ripening. *VaGH9B24* was not expressed in S3 and S4 stages but expressed in S1 and S2 stages.

AZs structure and cellulase activity of Vaccinium ashei

The cellular morphology of AZs at which fruit detachment takes place was examined by scanning electron microscopy (Fig. 9). As the fruit matured, a group of small, closely interconnected cells arranged in a rectangular shape in the AZs appeared to transform into a more rounded and elongated form with cell walls being less rigid (Fig. 9B). It was observed that cell division in AZs occurred adjacent to the phloem in the longitudinal profile of ethephon-treated fruits, as indicated an arrow, while a cleft only formed in control and ethephon-treated fruits (Fig. 9C). Notably, an indentation between the pedicel and fruit was deepened in ethephon-treated fruits, whereas it remarkably diminished in gibberellins-treated fruits due to the expansion of the surrounding cells.

Cellulase plays a crucial role in abscission process in many fruit crops such as apples, grapes, orange, and blackberries (Dal et al. 2020; Li et al. 2020; Merelo et al. 2017; Zhang et al. 2019). It was reported that abscission was accompanied by burst of reactive oxygen species (ROS), and that ethephon induced oxidative stress in abscission zone (Goldental-Cohen et al. 2017; Yang et al. 2015). Thus, activities of cellulose, ROS and malondialdehyde (MDA) levels, and relative conductivity in the AZs at the version stage were measured every seven days over 28 days during the fruit's maturation. As shown in Fig. 10A, cellulase activities in all three samples rapidly increased as the fruit ripened, with the highest activity observed in ethephon-treated AZs, showing a 118.26% increase relative to control at the fully ripe stage (S4 stage). On the other hand, gibberellins-treated AZs had the lowest cellulase activity. During fruit ripening, the levels of O_2^-, H_2O_2, MDA, and relative conductivity typically increased like cellulase activity. Ethephon treatment resulted in greater accumulation of O_2^- and H_2O_2 in the fruit AZs for 14–28 days. However, the application of gibberellins resulted in the suppression of the cellulase activity, O_2^-, H_2O_2, MDA, and relative conductivity in the AZs (Fig. 10A-E).

Discussion

It has been well documented that *GH9s* are involved in the breakdown of cell walls during plant growth and development including, but not limited to, fruit and leaf abscission, grain germination, pollen and seed dehiscence, cytokinesis, fruit softening, and senescence (Brummell et al. 1999; Campillo et al. 2012; Szyjanowicz et al. 2004; Xie et al. 2013; Yu et al. 2014; Zhou et al. 2006; Zuo et al. 2000). Due to their essential role in the organism's survival and fitness, *GH9* gene family is ubiquitously present in plants. This study identified 61 *VaGH9s* genes that can be grouped into three distinct clades based on the phylogenetic analysis of genome-wide sequence homology between the *Vaccinium ashei* and

Arabidopsis (Fig. 1, Table S1). Most VaGH9 proteins have a length that falls within the range of 417 to 694 aa, which is comparable to the range of GH9 proteins observed in other plants, such as 471–622 aa in *Populus L.*, 364–675 aa in *Arabidopsis*, and 441–694 aa in *Oryza sativa L.* (Du et al. 2015; Nunan et al. 2001; Xie et al. 2013). Proteins encoded by genes with a broad range of sequence similarity in the same family often have similar secondary and tertiary structures (Hayashi et al. 2005). Therefore, the similarity in structure and length across different species suggests that those GH9 proteins likely share similar functions as a result of divergent evolution from a common ancestor.

Our analyses of gene structure, along with conserved protein motifs and domains, revealed that most *VaGH9s* encode the highly conserved amino acid sequences with analogous number and distribution of motifs and domains, despite considerable variation in the number and length of introns and UTR among the 61 *VaGH9s* (Figs. 2 and 3). Similar observations were previously made in poplar and rice (Du et al. 2015; Xie et al. 2013). The UTRs are known to play an important role in post-transcriptional regulation of gene expression, such as controlling mRNA stability, localization, and translation (Mayr et al. 2019; Sangar et al. 2007). The presence or absence of specific regulatory elements within introns can also influence gene expression patterns (Jia et al. 2020). Gene with more and longer introns may have a slower transcription rate since splicing process takes longer to complete. This may result in lower mRNA levels and potentially lower protein levels, as well as a longer half-life of the mRNA in certain tissues or developmental stages. Moreover, longer introns may also contain regulatory elements that can affect gene expression, such as enhancers and silencers (Swinburne and Silver 2008). These elements can affect the transcription rate and alter the spatiotemporal gene expression patterns. On the other hand, genes with fewer and shorter introns may have a faster transcription rate since the splicing process is simpler and faster. This can result in higher mRNA levels and potentially higher protein levels, as well as a shorter half-life of the mRNA in other tissues or developmental stages. However, shorter introns may also have fewer regulatory elements, which can limit the ability of the gene to be regulated in response to environmental and developmental cues. Accordingly, the highly divergent structures of exon-intron and UTR present in *VaGH9s* may give rise to functionally distinct paralogs that differ in gene expression level and/or spatiotemporal patterns. This notion is further substantiated by the presence of the four categories of CARES involved in stress response, growth and development, hormone regulation, and transcription factors in the promoter regions of *VaGH9s*. Among many CAREs, the promoters of all 61 *VaGH9s* were found to have MYB in common. The MYB transcription factors are known to be involved in almost all aspects of plant development and metabolism by controlling the morphology and patterns of the cells (Li et al. 2019b; Wang et al. 2021a).

Besides the common glyco-hydro_9 domain, six other discrete domains were found in VaGH9 proteins (Fig. 3B). In this regard, three groups of proteins attracted our attention. First, VaGH9A1, whose gene was shown to be expressed in fruit AZs and its expression decreased as fruit ripened (Fig. 8), has three unique features in that its gene has the largest number of exon and introns and encodes hydrophobic proteins harboring three distinct domains, ferric reductase transmembrane component-like, FAD- and NAD-binding domains. Ferric reductase is known to be an integral membrane protein containing intra-membrane binding site for heme and cytoplasmic binding sites for nucleotide cofactors FAD and NAD, and this

enzyme is essential for plants to acquire soluble ferrous iron (Fe^{2+}) from soils (Riethoven et al. 2010). Ferric reductase 3 gene was shown to be necessary for correct iron localization in both the root and shoot of *Arabidopsis* plants (Robinson et al. 1999). Hence, *VaGH9A1* could also play a role in plant root and shoot growth and development. Secondly, *VaGH9B30* has two separate PME and PMEI domains, whereas *VaGHB7* has only PME domain involved in degradation of pectin that facilitates cell adhesion as the main component of the middle lamella of cell walls (Green et al. 2004). The *VaGH9B7* and *VaGHB30* genes, both of which lack ethylene-responsive CAREs (Fig. 4A), were not expressed in fruit AZs. Along this line, it was reported that the lack of a membrane-bound endo-1,4-β-glucanase may result in significant changes in pectin composition in the primary cell wall (Haas et al. 2021). The interplay between PME and PMEI was assumed to play a critical role in changing cell wall properties by regulating the extent of cell adhesion, cell wall porosity and elasticity in numerous biological processes (His et al. 2001). Thirdly, all VaGH9C5-8 proteins, which harbor non-catalytic C-terminal CBM49 domain, are very similar with respect to the size of proteins as well as the number and size of motifs and domains (Fig. 3). Except for *VaGH9C8* gene, *VaGH9C5-7* genes all have similar length and number of exon-introns and UTRs, as well as CARES (Figs. 2 and 4). They were all expressed and strongly induced by ethephon in fruit AZs, and *VaGH9C7* gene expression decreased as fruit ripened (Fig. 8). This result is consistent with the fact that CBMs are known to promote enzymatic hydrolysis of plant structural or storage polysaccharides by glycoside hydrolase through enhanced binding affinity (Wormit et al. 2018).

As for motif, it is notable that all the motifs are localized in the glycol_hydro_9 domain, irrespective of the clades. However, there are differences in the number and type of motifs between and within the clades (Fig. 3). For example, all VaGH9Cs in clade C harbor conserved motif 5, while VaGH9A1-7 proteins in clade A lack motif 5. The majority of VaGH9Bs in clade B have motifs 9–10, though VaGH9B subfamily has the largest members showing large differences in gene structure (Fig. 2). Due to the significant impact of motifs on protein function (Boraston et al. 2004), the presence or absence of a set of motifs within the glycoside hydrolase 9 domain of VaGH9s can lead to variations not only in the rate of catalytic activity and/or substrate affinity and specificity but also in the regulation of protein function. These unique sets of motifs may allow proteins to target specific substrate or respond to various signaling molecules. As previously reported (Cheng et al. 2019; Corbi-Verge and Kim 2016; Miller et al. 2018), some motifs could be subject to post-translational modifications or interact with regulatory proteins, leading to dissimilarities in the activation or inhibition of GH9s activity. Furthermore, different sets of motifs may also reflect changes in the protein's structural environment; for instance, if a GH is localized in a different subcellular compartment, it may require unique motifs to carry out its function in that environment. Overall, the presence of different sets of motifs in the catalytic domains in the members of GH9 family suggests that these proteins have diversified their functions over time, potentially to respond to dissimilar cellular contexts or to perform specialized tasks. Further studies to understand the differences in motif sets among GH9 family proteins would be useful for predicting their functional divergence and designing experiments to study their roles in biological processes.

The chromosomal localization and synteny analysis showed that *VaGH9s*, which are unevenly distributed across the chromosomes of *Vaccinium ashei*, share conserved collinear blocks. This suggests that *VaGH9* gene family has arisen from whole genome duplication event, which can lead to the presence of ortholog with similar functions between different genomes, and the paralogs within the same genome (Fig. 5, 6). The Ka/Ks values of *VaGH9* gene pairs were found to be less than 1 (Table S5), which implies that the duplicated genes could be evolved under negative selection pressure to retain their original function as a result of purifying selection. Similar observations were previously made in the *GH9* gene family of *Populus L.* and *Zea mays* (Buchanan et al. 2012; Du et al. 2015), as well as other gene families of COMT, ARF, and EXO70 in blueberry and grape (Li et al. 2022; Liu et al. 2021b; Wang et al. 2021b).

Considerable evidence suggests that GH9s have crucial functions in cell wall metabolism, particularly in relation to fruit ripening and abscission. For instance, the involvement of *CEL1*, the homolog of *GH9B1*, in regulating fruit maturation in strawberry has been demonstrated in several studies (Flors et al. 2007; Jara et al. 2019). Likewise, *FaEG1*, a member of GH9A, has been found to be involved in fruit ripening and organ abscission (Jara et al. 2019). In the present study, we identified 22 DEGs in fruit AZs tissues that could be assorted into five groups based on expression profiles in response to ethephon and gibberellins. Expression of *VaGH9B24* lacking ETH and GA CAREs (Fig. 4A) was not influenced by ethephon and gibberellins treatment but rather strongly declined after 24 h, while the other 21 genes were either strongly or weakly up- and/or down-regulated by ethephon and gibberellins treatment (Fig. 8A). Thus, it appears that *VaGH9B24* expression is entirely dependent on the progression of fruit development and its role is diminished during abscission process. Our qRT-PCR analysis of selected nine *VaGH9s* at four phenological stages of fruits (Fig. 8B) suggested their involvement in different stages of cell division process during abscission. Expression of *VaGH9A1* and *VaGH9C7* continuously declined, whereas that of *VaGH9B2* and *VaGH9C10* continuously increased in the fruit AZs during fruit maturation. This could be explained by the fact that *VaGH9A1* and *VaGH9C7* are involved in the pre-formation stage where AZs cell layers are differentiated, whereas *VaGH9B2* and *VaGH9C10* are involved in the separation stage where cell wall disassembly actively occurs. Along this line, our phylogenetic analysis (Fig. 1) showed that *VaGH9A1* was grouped with *AtGH9A1* and *PtrKOR1* (Fig. 1), both of which were found to be involved in the cellulose biosynthesis of both primary and secondary cell walls (Bhandari et al. 2006; Shani et al. 2006). *VaGH9B2* was grouped with *AtGH9B1* (*Arabidopsis* cellulase 1) that is thought to be involved in cell wall loosening that drives anisotropic cell elongation (Lipchinsky et al. 2013). Both *VaGH9C7* and *VaGH9C10* were grouped with *AtGH9C2* that was assumed to be engaged in modifying cell wall crystallinity (Glass et al. 2015). There appears to be no direct relationship between the number of motifs and the pattern of expression since *VaGH9B2* and *VaGH9C10* have 10 and 5 motifs, respectively (Fig. 3A). *VaGH9B24*, which has ABA-responsive element in its promoter region (Fig. 4A), was not expressed at S3 and S4 stages but expressed at S1 and S2 stages (Fig. 8C). *VaBH9B24* belongs to the same phylogenetic group as *AtGH9B8*, which is assumed to have a cell wall-organizing function and interact with ABA signaling terminator (Turco et al. 2017; Wang et al. 2020). *VaGH9A2, VaGH9B12*, and *VaGH9B14* were expressed at the highest level at the swelling (S2) stage, after which their expression gradually decreased during fruit maturation. *VaGH9A2* is classified in the same phylogenetic group as

VaGH9A1, while *VaGH9B12* and *VaGH9B14* are part of the group that includes *AtGH9B5*, which was believed to be involved in preserving the mechanical durability of the secondary cell wall (Glass et al. 2015). Thus, like *VaGH9A1* and *VaGH9C7*, the four *VaGH9s* (*B24*, *A2*, *B12*, and *B14*) also likely take part in the pre-formation stage of abscission, after which their expression decreases as the fruit matures.

It has been postulated that AZs are generated by the differentiation of the cells at a specific site into functionally competent cells that are sensitive to abscission signals (Estornell et al. 2013; Ma et al. 2021). Thus, we microscopically examined the fruit AZs tissues of *Vaccinium ashei* (Fig. 9). The result showed that epidermal cells in AZs are elongated, and that cell separation occurred in the site of fruit-pedicel junction, which was in agreement with the research on citrus and litchi (Li et al. 2019a; Merelo et al. 2017). However, when the fruits were treated with gibberellins, fruit abscission was inhibited and cell expansion occurred (Fig. 9), as previously reported on strawberry by Gu et al. (2019). It was observed that abscission was accompanied by the increased cell wall metabolism-related activities such as cellulose, ROS, relative conductivity, and MDA (Fig. 10). Similar observations were previously noted in mango, sweet cherries, and peach (Brahem et al. 2017; Chen et al. 2017; Gu et al. 2019; Huan et al. 2016; Ji et al. 2020; Luo et al. 2020).

Conclusions

In this study, we conducted a genome-wide analysis to identify *VaGH9* genes in *Vaccinium ashei* and grouped them into three distinct clades based on sequence homology. The study has also revealed that most *VaGH9s* encode highly conserved protein sequences with analogous motifs and domains, despite considerable variation in the number and length of introns and UTRs among 61 *VaGH9s*. This divergent structure may give rise to functionally distinct paralogs that differ in gene expression level and spatiotemporal patterns. The presence of four categories of CAREs associated with stress response, growth and development, hormone regulation, and transcription factors in the promoter regions of *VaGH9s* suggests that these genes may play a crucial role not only in plant growth and development but also stress and defense response. Moreover, this study has identified 22 *VaGH9s* that could play a role in the different stages of fruit abscission. The levels of cellulase activity and oxidative stress indicators rapidly increased in the fruit AZs tissues from S3 to S4 stage, with further increments observed after ethephon treatment and decrements observed after gibberellins treatment. These findings have significant implications for the breeding and improvement of fruit quality in *Vaccinium ashei* and other plants. However, further studies are needed to elucidate the precise roles and functions of *VaGH9s* in different tissues and under different environmental conditions.

Abbreviations

GH9: Glycosyl hydrolase family 9; AZ: Abscission zone; CMC: Carboxymethyl cellulose; WGD: Whole-genome duplication; COMT: Caffeic acid O-methyltransferases; ARF: Auxin responsive factor; EXO70: pivotal protein subunit of exocyst.

Declarations

Author Contributions W.Z. conceived and designed the experiments; Y.W. and T.L. performed the experiment and data analysis; Y.W., Y.X., Y.Z., F.L., T.L., X.L., B.W., and K.X. contributed to manuscript preparation; Y.W. and Y.Z. wrote original draft; W.Z. and S.H. performed the analysis with discussions. All authors have read and agreed to the published version of the manuscript.

Funding This work was supported by fund from Science and Technology Department of Zhejiang Province (2021C02066-6). We also gratefully acknowledge the financial support provided by Zhejiang A&F University (2010FR089).

Availability of data and materials

The *Vaccinium ashei* genome was downloaded from the (https://www.ncbi.nlm.nih.gov). Gene sequences of *Arabidopsis*, *Populus* L., *Vitis vinifera*, and *Citrus sinensis* were from (https://www.ncbi.nlm.nih.gov). *Vaccinium ashei* transcriptome data release channel (PRJNA899361).

Conflict of interest The authors declare that they have no competing interests.

References

1. Arseneault MH, Cline JA (2016) A review of apple preharvest fruit drop and practices for horticultural management. Sci Hortic 211:40-52. https://doi.org/10.1016/j.scienta.2016.08. 002
2. Bailey TL, Mikael B, Buske FA et al (2009) MEME SUITE: tools for motif discovery and searching. Nucleic Acids Res 37:W202-208. https://doi.org/10.1093/nar/gkp335
3. Bhandari S, Fujino T, Thammanagowda S et al (2006) Xylem-specific and tension stress-responsive coexpression of *KORRIGAN* endoglucanase and three secondary wall- associated cellulose synthase genes in aspen trees. Planta 224(4):828-837. https://doi. org/10.1007/s00425-006-0269-1
4. Boraston AB, Bolam DN, Gilbert HJ et al (2004) Carbohydrate-binding modules: fine-tuning polysaccharide recognition. Biochem J 382(Pt3):769-781. https://doi.org/10.1042/BJ2004 0892
5. Botton A, Ruperti B (2019) The Yes and No of the ethylene involvement in abscission. Plants (Basel) 8(6):187. https://doi.org/10.3390/plants8060187
6. Brahem M, Renard CM, Gouble B et al (2017) Characterization of tissue specific differences in cell wall polysaccharides of ripe and overripe pear fruit. Carbohydr Polym 156:152-164. https://doi.org/10.1016/j.carbpol.2016.09.019
7. Brummell DA, Hall BD, Bennett AB (1999) Anti-sense suppression of endo-1,4-B-glucanase *Cel2* mRNA accumulation increases the force required to break fruit abscission zones but does not affect fruit ripening. Plant Mol Biol 40(4):615-622. https://doi.org/10.1023/A:10062690 31452
8. Buchanan M, Burton RA, Dhugga KS et al (2012) Endo-(1,4)-β-glucanase gene families in the grasses: temporal and spatial co-transcription of orthologous genes. BMC Plant Biol 12:235. https://doi.org/10.1186/1471-2229-12-235

9. Campillo E, Gaddam S, Mettle-Amuah D et al (2012) A tale of two tissues: *AtGH9C1* is an endo-β-1,4-glucanase involved in root hair and endosperm development in *Arabidopsis*. PLoS One 7(11):e49363. https://doi.org/10.1371/journal.pone.0049363
10. Cantarel BL, Coutinho PM, Rancurel C et al (2009) The carbohydrate-active enzymes database (CAZy): an expert resource for glycogenomics. Nucleic Acids Res 37(Database issue) D233-238. https://doi.org/10.1093/nar/gkn663
11. Chen Y, Sun J, Lin H et al (2017) Paper-based 1-MCP treatment suppresses cell wall metabolism and delays softening of Huanghua pears during storage. J Sci Food Agric 97(8):2547-2552. https://doi.org/10.1002/jsfa.8072
12. Chen S, Zhou Y, Chen Y et al (2018) Fastp: an ultra-fast all-in-one FASTQ preprocessor. Bioinformatics 34(17):i884-i890. https://doi.org/10.1093/bioinformatics/bty560
13. Chen C, Chen H, Zhang Y et al (2020) TBtools: an integrative toolkit developed for interactive analyses of big biological data. Mol Plant 13(8):1194-1202. https://doi.org/10.1016/ j.molp.2020.06.009
14. Cheng A, Grant CE, Noble WS et al (2019) MoMo: discovery of statistically significant post-translational modification motifs. Bioinformatics 35(16):2774-2782. https://doi.org/10. 1093/bioinformatics/bty1058
15. Chou KC, Shen HB (2010) Cell-PLoc 2.0: an improved package of web-servers for predicting subcellular localization of proteins in various organisms. Natural Science 2: 1090-1103. https://doi.org/10.1038/nprot.2007.494
16. Colle M, Leisner CP, Wai CM et al (2019) Haplotype- phased genome and evolution of phytonutrient pathways of tetraploid blueberry. Gigascience 8(3):giz012. https://doi.org/10. 1093/gigascience/giz012
17. Corbi-Verge C, Kim PM (2016) Motif mediated protein-protein interactions as drug targets. Cell Commun Signal 14:8. https://doi.org/10.1186/s12964-016-0131-4
18. Dal SS, Tucker MR, Tan HT et al (2020) Auxin treatment of grapevine (*Vitis vinifera* L.) berries delays ripening onset by inhibiting cell expansion. Plant Mol Biol 103:91-111. https://doi. org/10.1007/s11103-020-00977-1
19. Davidson KT, Zhu Z, Balabanov D et al (2018) Beyond conventional medicine-A look at blueberry, a cancer-fighting superfruit. Pathol Oncol Res 24(4):733-738. https://doi.org/10. 1007/s12253-017-0376-2
20. Del C E, Gaddam S, Mettle-Amuah D et al (2012) A tale of two tissues: *AtGH9C1* is an endo-β-1,4-glucanase involved in root hair and endosperm development in *Arabidopsis*. PLoS One 7(11):e49363. https://doi.org/10.1371/journal.pone.0049363
21. Del A R, Branco C, Arenas J et al (2021) Analysis of selection in protein-coding sequences accounting for common biases. Brief Bioinform 22(5): bbaa431. https://doi.org/10.1093/ bib/bbaa431
22. Dheilly E, Gall SL, Guillou MC et al (2016) Cell wall dynamics during apple development and storage involves hemicellulose modifications and related expressed genes. BMC Plant Biol 16(1):201.

https://doi.org/10.1186/s12870-016-0887-0

23. Du Q, Wang L, Yang X et al (2015) Populus endo-β-1,4-glucanases gene family: genomic organization, phylogenetic analysis, expression profiles and association mapping. Planta 241(6):1417-1434. https://doi.org/10.1007/s00425-015-2271-y
24. Estornell LH, Agustí J, Merelo P et al (2013) Elucidating mechanisms underlying organ abscission. Plant Sci 199-200:48-60. https://doi.org/10.1016/j.plantsci.2012.10.008
25. Fidelibus MW, Petracek P, McArtney S (2022) Jasmonic acid activates the fruit-pedicel abscission zone of '*thompson seedless*' grapes, especially with co-application of 1-aminocyclopropane- 1-carboxylic acid. Plants (Basel) 11(9):1245. https://doi.org/10.3390/plants11091245
26. Flors V, Leyva Mde L, Vicedo B et al (2007) Absence of the endo-beta-1,4-glucanases *Cel1* and *Cel2* reduces susceptibility to *Botrytis cinerea* in tomato. Plant J 52(6):1027-1040. https://doi.org/10.1111/j.1365-313X.2007.03299.x
27. Freeling, M (2009) Bias in plant gene content following different sorts of duplication: tandem, whole-genome, segmental, or by transposition. Annu Rev Plant Biol 60:433-453. https://doi.org/10.1146/annurev.arplant.043008.092122
28. Ghose TK (2013) Measurement of cellulase activities. Pure Appl Chem 59(2):257-268. https://doi.org/10.1351/pac198759020257
29. Glass M, Barkwill S, Unda F et al (2015) Endo-β-1,4-glucanases impact plant cell wall development by influencing cellulose crystallization. J Integr Plant Biol 57(4):396-410. https://doi.org/10.1111/jipb.12353
30. Gray M, Linton SM, Allardyce BJ (2018) cDNA sequences of GHF9 endo-β-1,4-glucanases in terrestrial *Crustacea*. Gene 642:408-422. https://doi.org/10.1016/j.gene.2017.11.030
31. Green LS, Rogers EE (2004) *FRD3* controls iron localization in *Arabidopsis*. Plant Physiol 136(1):2523-2531. https://doi.org/10.1104/pp.104.045633
32. Goldental-Cohen S, Burstein C, Biton I et al (2017) Ethephon induced oxidative stress in the olive leaf abscission zone enables development of a selective abscission compound. BMC Plant Biol 17(1):87. https://doi.org/10.1186/s12870-017-1035-1
33. Gu T, Jia S, Huang X et al (2019) Transcriptome and hormone analyses provide insights into hormonal regulation in strawberry ripening. Planta 250(1):145-162. https://doi.org/10.1007/ s00425-019-03155-w
34. Haas KT, Wightman R, Peaucelle A et al (2021) The role of pectin phase separation in plant cell wall assembly and growth. Cell Surf 7:100054. https://doi.org/10.1016/j.tcsw.2021.100054
35. Hayashi T, Yoshida K, Park YW et al (2005) Cellulose metabolism in plants. Int Rev Cytol 247:1-34. https://doi.org/10.1016/S0074-7696(05)47001-1
36. He S, Yu H, Gu Y (2009) Prospects and problems of blueberry growing in China. Acta Horticul (810):61-64. https://doi.org/10.17660/ActaHortic.2009.810.3

37. His I, Driouich A, Nicol F et al (2001) Altered pectin composition in primary cell walls of korrigan, a dwarf mutant of Arabidopsis deficient in a membrane-bound endo-1,4-beta- glucanase. Planta 212(3):348-358. https://doi.org/10.1007/s004250000437
38. Hu B, Jin JP, Guo AY et al (2015) GSDS 2.0: an upgraded gene feature visualization server. Bioinformatics 31(8):1296-1297. https://doi.org/10.1093/ bioinfor- matics/btu817
39. Huan C, Jiang L, An X et al (2016) Potential role of reactive oxygen species and antioxidant genes in the regulation of peach fruit development and ripening. Plant Physiol Biochem 104:294- 303. https://doi.org/10.1016/j.plaphy.2016.05.013
40. Jaillon O, Aury J-M, Noel B et al (2007) The grapevine genome sequence suggests ancestral hexaploidization in major angiosperm phyla. Nature 449:463. https://doi.org/10.1038/nature 06148
41. Jambunathan N (2010) Determination and detection of reactive oxygen species (ROS), lipid peroxidation, and electrolyte leakage in plants. Methods Mol Biol 639:292-298. https://doi.org/10.1007/978-1-60761-702-018
42. Jara K, Castro RI, Ramos P et al (2019) Molecular insights into *FaEG1*, a strawberry endoglucanase enzyme expressed during strawberry fruit ripening. Plants (Basel) 8(6):140. https://doi.org/10.3390/plants8060140
43. Ji Y, Hu W, Liao J et al (2020) Effect of atmospheric cold plasma treatment on antioxidant activities and reactive oxygen species production in postharvest blueberries during storage. J Sci Food Agric 100(15):5586-5595. https://doi.org/10.1002/jsfa.10611
44. Jia L, Mao Y, Ji Q et al (2020) Decoding mRNA translatability and stability from the 5' UTR. Nat Struct Mol Biol 27(9):814-821. https://doi.org/10.1038/ s41594-020-0465-x
45. Kalaitzis P, Hong SB, Solomos T et al (1999) Molecular characterization of a tomato endo-beta-1,4-glucanase gene expressed in mature pistils, abscission zones and fruit. Plant Cell Physiol 40(8):905-908. https://doi.org/10.1093/oxfordjournals.pcp.a029621
46. Korbinian S, Stephan O, Felix O et al (2011) Reference-guided assembly of four diverse *Arabidopsis thaliana* genomes. Proc Natl Acad Sci USA 108(25):10249-10254. https://doi.org/10.1073/pnas.1107739108
47. Kulkarni KP, Vorsa N, Natarajan P et al (2020) Admixture analysis using genotyping-by- sequencing reveals genetic relatedness and parental lineage distribution in highbush blueberry genotypes and cross derivatives. Int J Mol Sci 22(1):163. https://doi.org/10.3390/ ijms22010163
48. Kumar S, Stecher G, Tamura K (2016) MEGA7: Molecular evolutionary genetics analysis version 7.0 for bigger datasets. Mol Biol Evol 33(7):1870-1874. https://doi.org/10.1093/mol bev/msw054
49. Kumar S, Stecher G, Li M et al (2018) MEGA X: Molecular evolutionary genetics analysis across computing platforms. Mol Biol Evol 35:1547-1549. https://doi.org/10.1093/molbev/msy096
50. Lescot M, Déhais P, Thijs G et al (2002) PlantCARE, a database of plant cis-acting regulatory elements and a portal to tools for in silico analysis of promoter sequences. Nucleic Acids Res 30(1):325-327. https://doi.org/10.1093/nar/30.1.325

51. Li T, Zhang J, Zhu H et al (2016) Proteomic analysis of differentially expressed proteins involved in peel senescence in harvested mandarin fruit. Front Plant Sci 7:725. https://doi.org/10.3389/fpls.2016.00725
52. Li C, Zhao M, Ma X et al (2019a) The HD-Zip transcription factor *LcHB2* regulates litchi fruit abscission through the activation of two cellulase genes. J Exp Bot 70(19):5189-5203. https://doi.org/10.1093/jxb/erz276
53. Li J, Han G, Sun C et al (2019b) Research advances of MYB transcription factors in plant stress resistance and breeding. Plant Signal Behav14(8):1613131. https://doi.org/10.1080/15592324.2019.1613131
54. Li C, Zhang J, Ge Y et al (2020) Postharvest acibenzolar-S-methyl treatment maintains storage quality and retards softening of apple fruit. J Food Biochem 44(3):e13141. https://doi.org/10.1111/jfbc.13141
55. Li X, Zhang X, Shi T et al (2022) Identification of *ARF* family in blueberry and its potential involvement of fruit development and pH stress response. BMC Genomics 23(1):329. https://doi.org/10.1186/s12864-022-08556-y
56. Lipchinsky A (2013) How do expansins control plant growth? A model for cell wall loosening via defect migration in cellulose microfibrils. Acta physiol plant. 35:3277-3284. https://doi.org/10.1007/s11738-013-1341-7
57. Liu B, Wang K, Shu X et al (2019) Changes in fruit firmness, quality traits and cell wall constituents of two highbush blueberries (*Vaccinium corymbosum* L.) during postharvest cold storage. Sci Hortic 246:557-562. https://doi.org/10.1016/j.scienta.2018.11.042
58. Liu S, Wang Z, Zhu R et al (2021a) Three differential expression analysis methods for RNA sequencing: limma, EdgeR, DESeq2. J Vis Exp (175). https://doi:10.3791/62528.
59. Liu Y, Wang Y, Pei J et al (2021b) Genome-wide identification and characterization of *COMT* gene family during the development of blueberry fruit. BMC Plant Biol 21(1):5. https://doi.org/10.1186/s12870-020-02767-9
60. Livak KJ, Schmittgen TD (2001) Analysis of relative gene expression data using real-time quantitative PCR and the $2^{-\Delta\Delta CT}$ method. Methods 25(4):402-408. https://doi.org/10.1006/meth.2001.1262
61. Luo Y, Ge C, Ling Y et al (2020) ABA and sucrose co-regulate strawberry fruit ripening and show inhibition of glycolysis. Mol Genet Genomics 295(2):421-438. https://doi.org/10. 1007/s004 38-019-01629-w
62. Luo L, Bai J, Yuan S et al (2022) Genome wide identification and characterization of wheat GH9 genes reveals their roles in pollen development and anther dehiscence. Int J Mol Sci 23(11):6324. https://doi.org/10.3390/ijms23116324
63. Ma C, Jiang CZ, Gao JP (2021) Regulatory mechanisms underlying activation of organ abscission. Annual Plant Reviews Online 4:27-56. https://doi.org/10.1002/9781119312994.apr0741

64. Main D S, Jung Sook (2018) Genome Database for *Vaccinium*. Main Lab Bioinformatics, Washington State University. https://data.nal.usda.gov/dataset/genome-database-vaccinium.
65. Mayr C (2019) What Are 3' UTRs Doing? Cold Spring Harb Perspect Biol. 11(10):a034728. doi: 10.1101/cshperspect.a034728
66. Mercado JA, Trainotti L, Jiménez-Bermúdez L et al (2010) Evaluation of the role of the endo-β-(1,4)-glucanase gene *FaEG3* in strawberry fruit softening. Postharvest Biol Technol 55(1):8-14. https://doi.org/10.1016/j.postharvbio.2009.08.004
67. Merelo P, Agustí J, Arbona V et al (2017) Cell wall remodeling in abscission zone cells during ethylene-promoted fruit abscission in Citrus. Front Plant Sci 8:126. https://doi.org/ 10.3389/fpls.2017.00126
68. Miller CJ, Turk BE (2018) Homing in: mechanisms of substrate targeting by protein kinases. Trends Biochem Sci 43(5):380-394. https://doi.org/10.1016/j.tibs.2018.02.009
69. Mistry J, Chuguransky S, Williams L et al (2021) Pfam: the protein families database in 2021. Nucleic Acids Res 49(D1):D412-D419. https://doi.org/10.1093/nar/gkaa913
70. Nunan KJ, Davies C, Robinson SP et al (2001) Expression patterns of cell wall-modifying enzymes during grape berry development. Planta 214(2):257-264. https://doi.org/10.1007/ s004250100609
71. Patharkar OR, Walker JC (2018) Advances in abscission signaling. J Exp Bot 69(4):733-740. https://doi.org/ 10.1093/jxb/erx256.
72. Priya S, Shiv KM, Laxmipriya P et al (2022) The JA pathway is rapidly down-regulated in petal abscission zones prior to flower opening and affects petal abscission in fragrant roses during natural and ethylene-induced petal abscission. Sci Hortic 300:111072. https://doi.org/ 10.1016/j.scienta.2022.111072
73. Potter SC, Luciani A, Eddy SR et al (2018) HMMER web server: 2018 update. Nucleic Acids Res 46(W1):W200-204. https://doi.org/10.1093/nar/gky448
74. Qian C, He Z, Zhao Y et al (2013) Maturity-dependent chilling tolerance regulated by the antioxidative capacity in postharvest cucumber (*Cucumis sativus L.*) fruits. J Sci Food Agric 93(3):626-633. https://doi.org/10.1002/jsfa.5858
75. Qiu ZL, Wen Z, Yang K et al (2020) Comparative proteomics profiling illuminates the fruitlet abscission mechanism of sweet cherry as induced by embryo abortion. Int J Mol Sci 21(4):1200. https://doi.org/10.3390/ijms21041200
76. Riethoven JJ (2010) Regulatory regions in DNA: promoters, enhancers, silencers, and insulators. Methods Mol Biol 674:33-42. https://doi.org/10.1007/978-1-60761-854-6_3
77. Roberts JA, Elliott KA, Gonzalez-Carranza ZH (2002) Abscission, dehiscence, and other cell separation processes. Annu Rev Plant Biol 53:131-158. https://doi.org/10.1146/annurev.ar plant.53.092701.180236
78. Robinson NJ, Procter CM, Connolly EL et al (1999) A ferric-chelate reductase for iron uptake from soils. Nature 397(6721):694-697. https://doi.org/10.1038/17800

79. Sabbione A, Daurelio L, Vegetti A et al (2019) Genome-wide analysis of *AGO*, *DCL* and *RDR* gene families reveals RNA-directed DNA methylation is involved in fruit abscission in *Citrus sinensis*. BMC Plant Biol 19(1):401. https://doi.org/10.1186/s12870-019-1998-1

80. Sangar V, Blankenberg DJ, Altman N et al (2007) Quantitative sequence-function relationships in proteins based on gene ontology. BMC Bioinformatics 8:294. https://doi.org/10.1186/ 1471-2105-8-294

81. Sawicki M, Ait Barka E, Clement C et al (2015) Cross-talk between environmental stresses and plant metabolism during reproductive organ abscission. J Exp Bot 66(7):1707-1719. https://doi.org/10.1093/jxb/eru533

82. Schmitz RJ, Grotewold E, Stam M (2022) Cis-regulatory sequences in plants: Their importance, discovery, and future challenges. Plant Cell 34(2):718-741. https://doi.org/10.1093/plcell/ koab281

83. Shani Z, Dekel M, Roiz L et al (2006) Expression of endo-1,4-beta-glucanase (cel1) in *Arabidopsis thaliana* is associated with plant growth, xylem development and cell wall thickening. Plant Cell Rep 25(10):1067-1074. https://doi.org/10.1007/s00299-006-0167-9

84. Swinburne IA, Silver PA (2008) Intron delays and transcriptional timing during development. Dev Cell 14(3):324-330. https://doi.org/10.1016/j.devcel.2008.02.002

85. Szyjanowicz PM, McKinnon I, Taylor NG et al (2004) The irregular xylem 2 mutant is an allele of korrigan that affects the secondary cell wall of *Arabidopsis thaliana*. Plant J 37(5):730-740. https://doi.org/10.1111/j.1365-313X.2003.02000.x

86. Trapnell C, Roberts A, Goff L et al (2012) Differential gene and transcript expression analysis of RNA-seq experiments with TopHat and Cufflinks. Nat Protoc 7(3):562-578. https://doi. org/10.1038/nprot1014-2513a

87. Turco GM, Kajala K, Kunde-Ramamoorthy G, et al (2017) DNA methylation and gene expression regulation associated with vascularization in *Sorghum bicolor*. New Phytol 214(3):1213-1229. https://doi: 10.1111/nph.14448

88. Tuskan GA, Difazio S, Jansson S et al (2006) The genome of black cottonwood, *Populus trichocarpa* (Torr & Gray). Science 313(5793):1596-1604. https://www.srs.fs.usda.gov/ pubs/24556

89. Urbanowicz BR, Bennett AB, Del CE et al (2007) Structural organization and a standardized nomenclature for plant endo-1,4-beta-glucanases (cellulases) of glycosyl hydrolase family 9. Plant Physiol 144(4):1693-1696. https://doi.org/10. 1104/pp.107.102574

90. Vashisth T, Johnson LK, Malladi A (2011) An efficient RNA isolation procedure and identification of reference genes for normalization of gene expression in blueberry. Plant Cell Rep 30(12):2167-2176. https://doi.org/10.1007/s00299-011-1121-z

91. Vashisth T and Malladi A (2013) Fruit detachment in rabbiteye blueberry: abscission and physical separation. J Amer Soc Hort Sci 138(2):95-101. https://doi.org/10.21273/JASHS. 138.2.95

92. Vashisth T, NeSmith DS, Malladi A (2015) Anatomical and gene expression analyses of two blueberry genotypes displaying differential fruit detachment. J Amer Soc Hort Sci 140(6): 620-626. https://doi.org/10.21273/JASHS.140.6.620

93. Wang Y, Tang H, Debarry JD et al (2012) MCScanX: a toolkit for detection and evolutionary analysis of gene synteny and collinearity. Nucleic Acids Res 40(7):e49. https://doi.org/10.10 93/nar/gkr1293
94. Wang J, Chen D, Lei Y et al (2014) Citrus sinensis annotation project (CAP): a comprehensive database for sweet orange genome. PLoS One 9(1):e87723. https://doi.org/10.1371/ journal.pone.0087723
95. Wang F, Zheng Z, Yuan Y et al (2019) Identification and characterization of HAESA-like genes involved in the fruitlet abscission in Litchi. Int J Mol Sci 20(23):5945. https:// doi.org/10.3390/ijms20235945
96. Wang Z, Ren Z, Cheng C, et al (2020) Counteraction of ABA-Mediated Inhibition of Seed Germination and Seedling Establishment by ABA Signaling Terminator in *Arabidopsis*. Mol Plant 13(9):1284-1297. https://doi: 10.1016/j.molp.2020.06.011.
97. Wang X, Niu Y, Zheng Y (2021a) Multiple functions of MYB transcription factors in abiotic stress responses. Int J Mol Sci 22(11):6125. https://doi.org/10.3390/ijms22116125
98. Wang H, Ma ZH, Mao J et al (2021b) Genome-wide identification and expression analysis of the *EXO70* gene family in grape (*Vitis vinifera L*). Peer J 9:e11176. https://doi.org/ 10.7717/peerj.11176
99. Wormit A, Usadel B (2018) The multifaceted role of pectin methylesterase inhibitors (PMEIs). Int J Mol Sci 19(10):2878. https://doi.org/10.3390/ijms19102878
100. Xie G, Yang B, Xu Z et al (2013) Global identification of multiple *OsGH9* family members and their involvement in cellulose crystallinity modification in rice. PLoS One 8(1):e50171. https://doi.org/10.1371/ journal. pone.0050171
101. Yang Z, Zhong X, Fan Y et al (2015) Burst of reactive oxygen species in pedicel-mediated fruit abscission after carbohydrate supply was cut off in longan (*Dimocarpus longan*). Front Plant Sci 6:360. https://doi.org/10.3389/fpls.2015.00360
102. Yu L, Chen H, Sun J et al (2014) *PtrKOR1* is required for secondary cell wall cellulose biosynthesis in *Populus L.* Tree Physiol. 34(11):1289-300. https://doi.org/10.1093/ treephys/ tpu020
103. Zhang C, Xiong Z, Yang H et al (2019) Changes in pericarp morphology, physiology and cell wall composition account for flesh firmness during the ripening of blackberry (*Rubus spp.*) fruit. Sci Hortic 250:59-68. https://doi.org/10.1016/j.scient a.2019.02.015
104. Zhou HL, He SJ, Cao YR et al (2006) *OsGLU1*, a putative membrane-bound endo-1,4-beta- D-glucanase from rice, affects plant internode elongation. Plant Mol Biol 60(1):137-151. https://doi.org/10.1007/s11103-005-2972-x
105. Zuo J, Niu QW, Nishizawa N et al (2000) *KORRIGAN*, an *Arabidopsis* endo-1,4-beta-glucanase, localizes to the cell plate by polarized targeting and is essential for cytokinesis. Plant Cell 12(7):1137-1152. https://doi.org/10.1105/tpc.12.7.1137

Figures

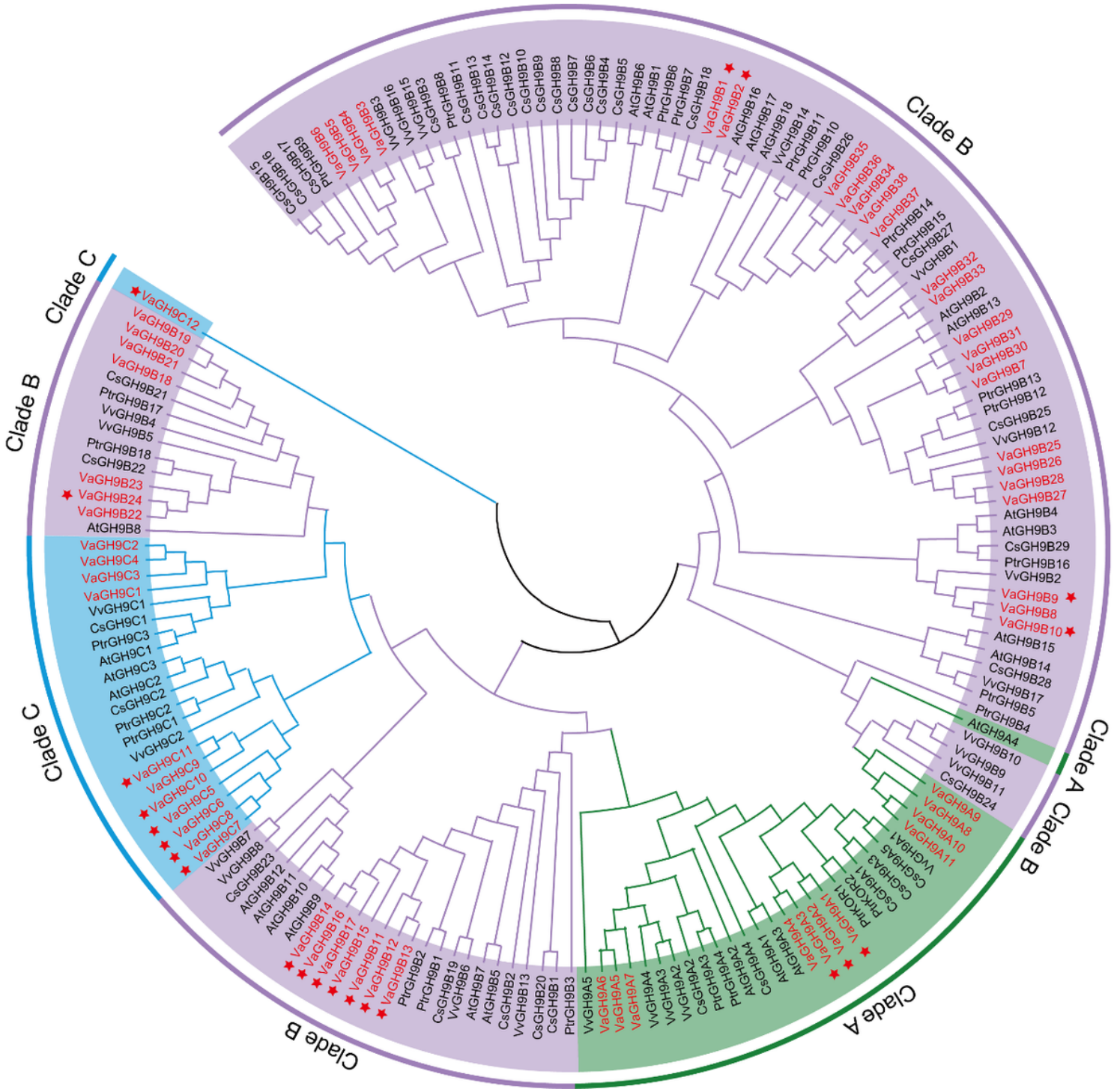

Figure 1

Phylogenetic trees of the GH9s proteins from rabbiteye blueberry, *Arabidopsis*, poplar, grape, and orange. The complete amino acid sequences of 61 *Vaccinium ashei*, 25 *Arabidopsis*, 25 *Populus L.*, 24 *Vitis vinifera*, and 39 *Citrus sinensis* GH9 proteins were retrieved from NCBI (www.ncbi.nlm.nih.gov) database, aligned and compared with ClustalX, and the phylogenetic trees were constructed using MEGA7.0 according to the neighbor-joining method with 1000 bootstrap replicates. The GH9s of *Arabidopsis*, *Populus L.*, *Vitis vinifera*, *Citrus sinensis*, and *Vaccinium ashei*were prefixed with At, Ptr, Vv, Cs, and Va, respectively. Different colors of the tree lines represent different clades. The branches sharing the same

color are in the same subfamily. The stars denote differentially expressed genes according to the transcriptome sequencing of the fruit abscission zones in the veraison stage after ethylene and gibberellins treatment.

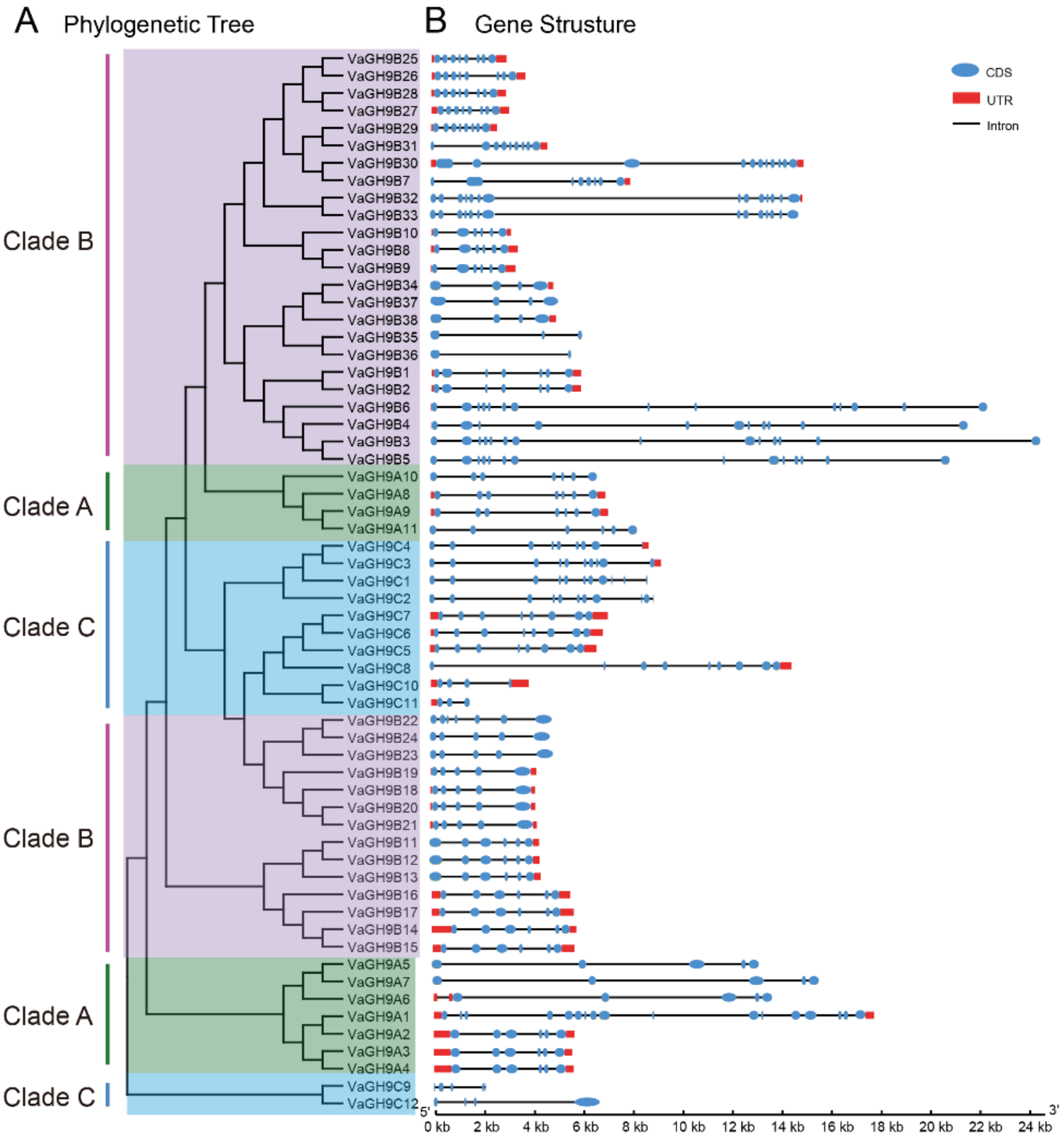

Figure 2

The polygenetic relationship and gene structure of the *VaGH9s* in *Vaccinium ashei*. **A** The phylogenetic tree was constructed using MEGA7.0 according to the NL method. **B** Exon-intron structures of the 61 putative *VaGH9* genes. The exons are shown by blue rectangle, and the introns are represented by black lines. Red rectangle refers to the untranslated region of mRNA upstream of start codon (5'-UTR) and downstream of stop codon (3'-UTR).

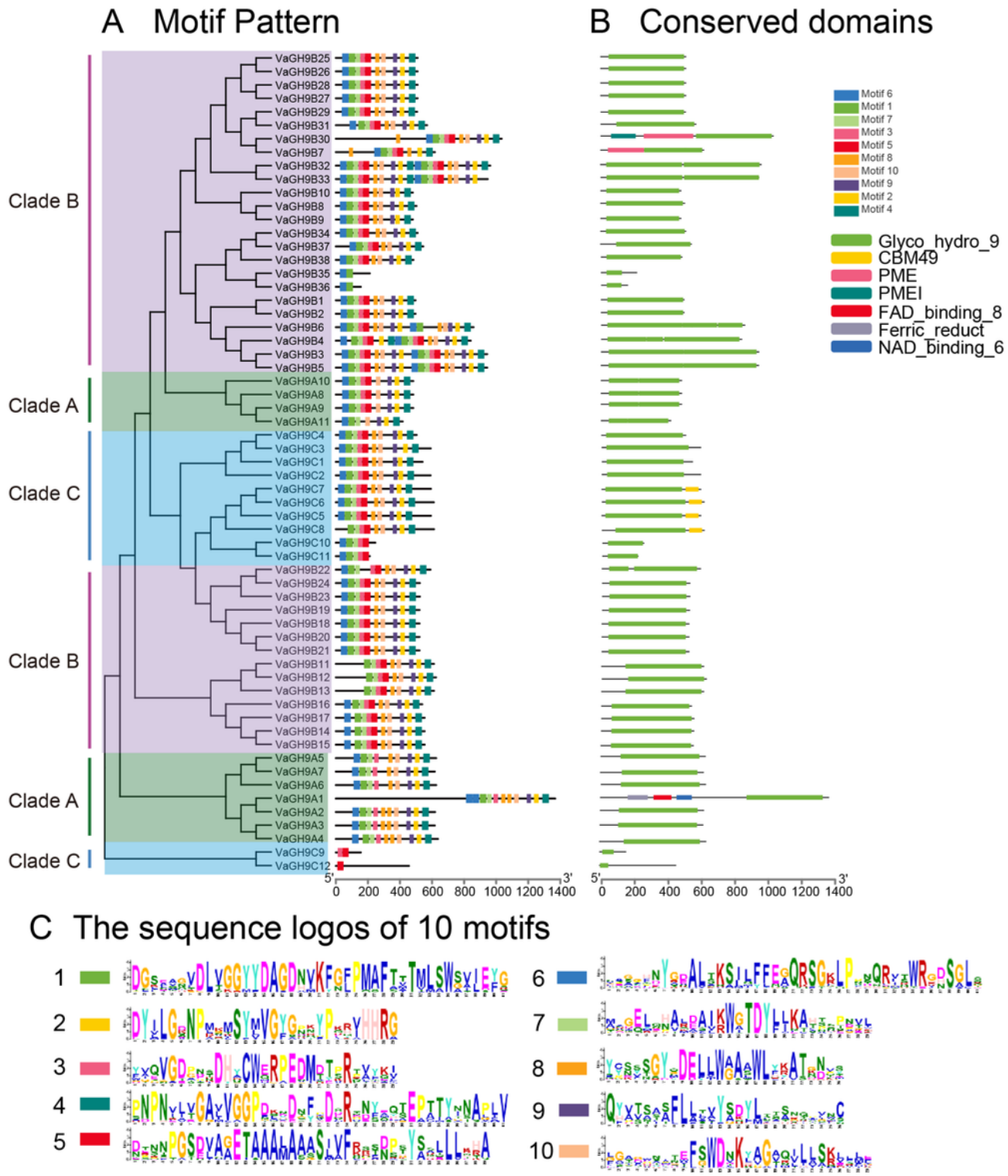

Figure 3

Conserved domain and motif compositions of VaGH9 proteins. **A** The phylogenetic tree of VaGH9 proteins, and three groups are clustered (A, B, C). Ten motifs are displayed in rectangles with different colors and are annotated in Table S2. **B** The domain composition of VaGH9s. Green, yellow, pink, blue, red, purple, and blue rectangles represent the Glyco_hydro_9 domain (IPR001701), CBM49 domain (IPR019028), PME domain (IPR000070), PMEI domain (IPR006501), FAD_binding_8 domain (IPR013112), Ferric_reduct domain (IPR013130), and NAD_binbing_6 domain (IPR036291), respectively. Glyco_hydro_9, glycosyl hydrolase 9; CBM49, carbohydrate binding module family 49; PME, pectin methylesterase; PEMEI, pectin methylesterase inhibitor; FAD, flavin adenine dinucleotide; Ferric_reduct, ferric reductase transmembrane component-like; NAD, nicotinamide adenine dinucleotide. The numbers under the horizontal lines refer to amino acids with 5'-NH_2 and 3'-COOH termini of proteins. **C** The sequence logos of 10 motifs.

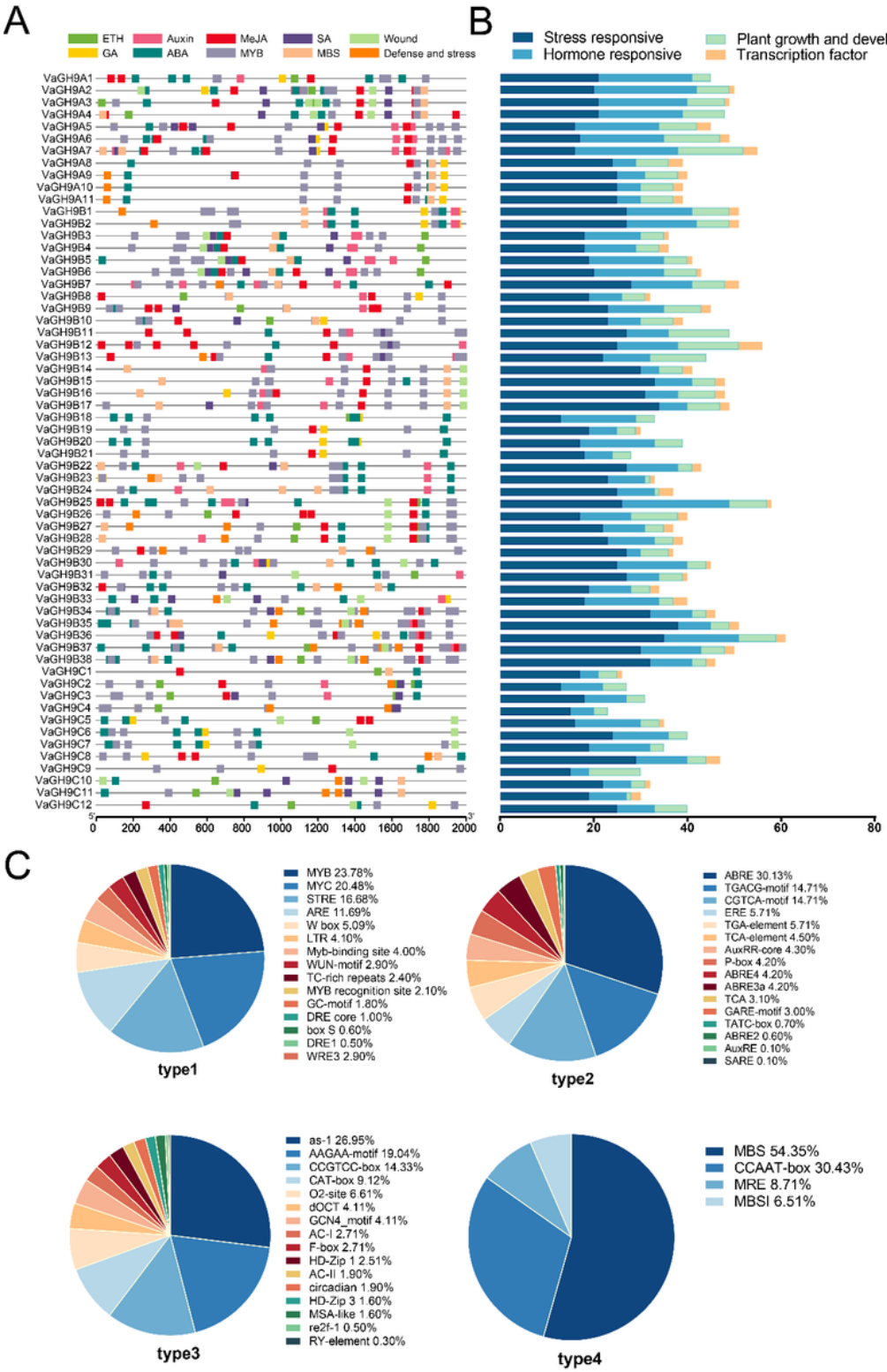

Figure 4

Analysis of *cis*-regulatory element distribution in the *VaGH9* promoters. **A**The *cis*-elements in the *VaGH9s* were marked by different colors. **B**The number of *cis*-elements numbers in four categories; dark blue histograms (type1), stress responses; blue histograms (type 2), plant hormone regulation; cyan histograms (type 3), growth and development; and orange histograms (type 4), transcription factor. **C** The proportions of distinct *cis*-elements from four categories

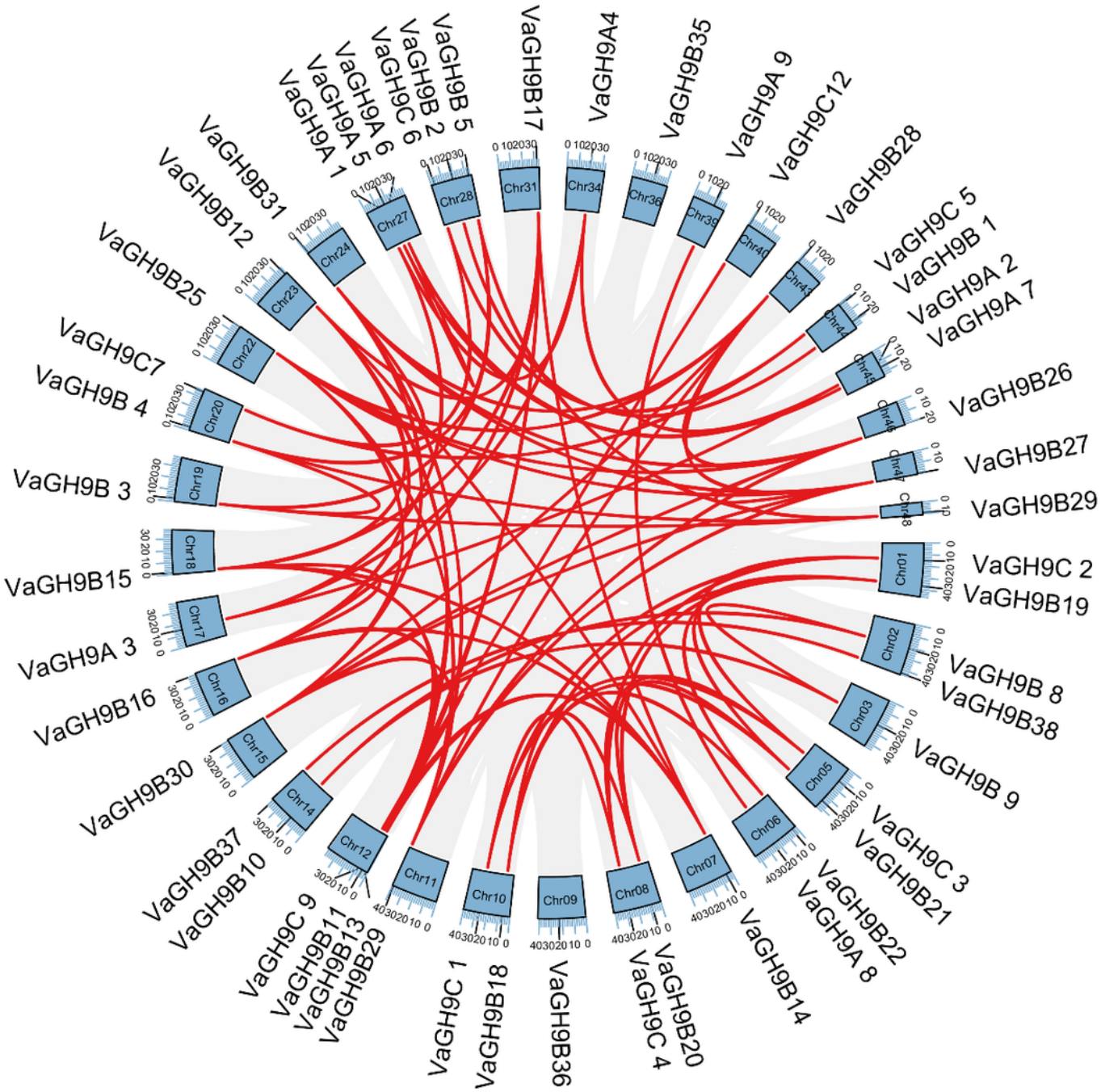

Figure 5

A Circos plot showing distribution of *VaGH9* genes among 34 scaffold chromosomes and synteny analysis in *Vaccinium ashei* genome. The annotations on the fragments represent different chromosomes, and the numbers in the outermost circle denote the positions on the corresponding chromosomes. The approximate position of each *VaGH9*gene is marked with a short black line. The *VaGH9s* paralogs in *Vaccinium ashei* are mapped to their respective locations in the circular diagram.

The red and grey lines refer to the segmental duplication pairs between the *VaGH9s*and the segmental duplication pairs in the whole genome, respectively.

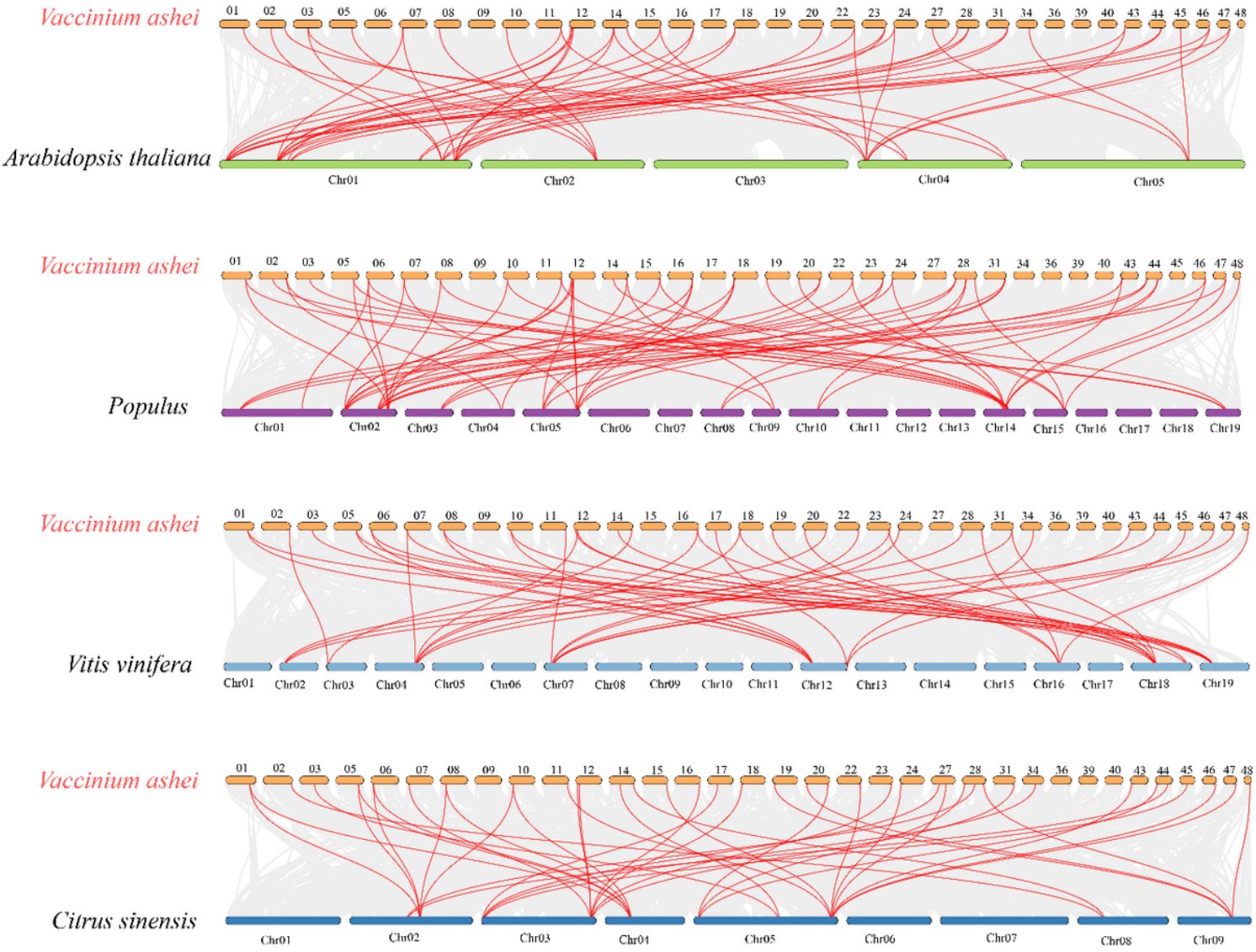

Figure 6

Synteny analysis of *GH9* genes between *Vaccinium ashei* and other four species. Gray lines in the background indicate the collinear blocks within *Vaccinium ashei* and other plant genomes, whereas the red lines highlight the syntenic *GH9* gene pairs.

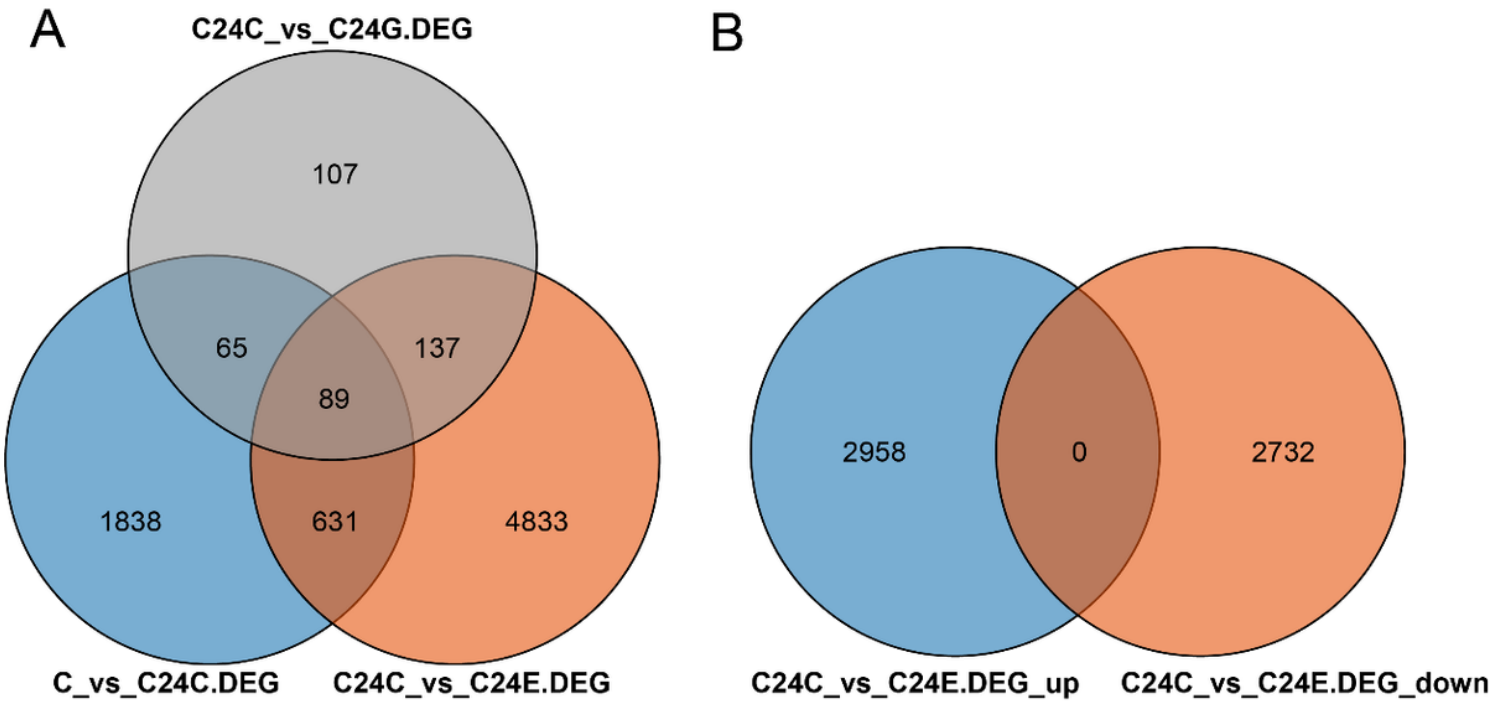

Figure 7

Vaccinium ashei differentially expressed genes in the Ctrl, ethylene, and gibberellins samples. **A** Venn diagram of the intersection between the Ctrl, ethylene, and gibberellins DEGs. **B**Venn diagram of the intersection between the ethephon treatment significantly up-regulated DEGs and down-regulated DEGs.

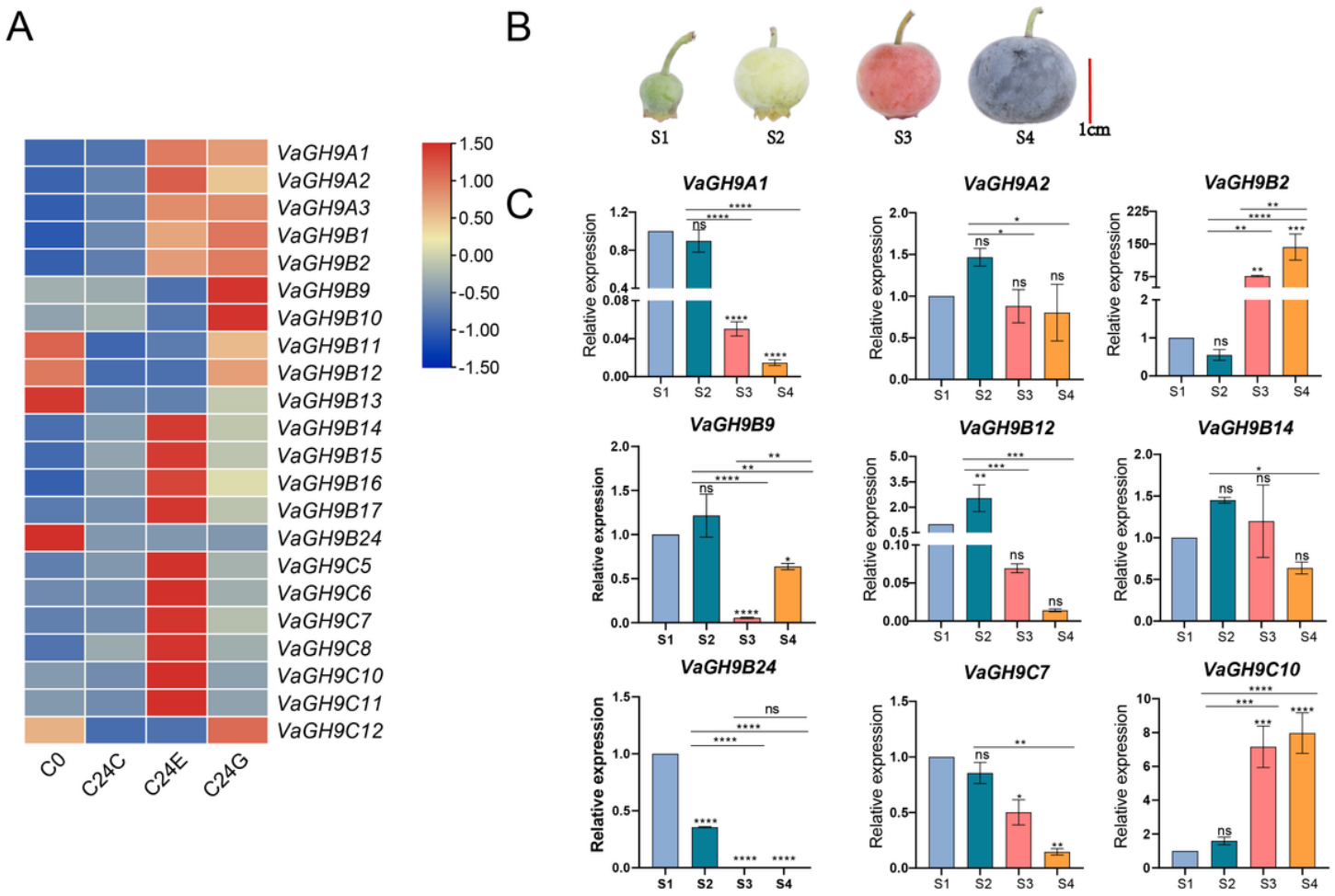

Figure 8

Expression analysis of *VaGH9* genes during fruit development. **A** Heatmap of differentially expressed *VaGH9* genes in AZs of rabbiteye blueberries treated with ethephon and gibberellins at the veraison stage. The color scales with Z scores beside the heat map indicate gene expression levels. The low and high transcript abundance are indicated by blue and red color, respectively. C0, 0-h untreated control; C24C, 24-h untreated control; C24E, 24-h treated ethephon; C24G, 24-h treated gibberellins. **B** Photograph of fruits at four developmental stages (fruitlet stage (S1), swelling stage (S2), veraison stage (S3), and fully ripe stage (S4)). The scale bar indicates 1 cm. **C** Expression patterns of *VaGH9s* in AZs during fruit development. Total RNAs were extracted at the four developmental stages. Data were normalized against an internal control UBQ3b, and the expression level at S1 stage was set as 1. Error bars indicate standard deviation, and asterisks indicate significant differences between the control and treatments, *P<0.05, **P<0.01, ***P<0.001, ****P<0.0001.

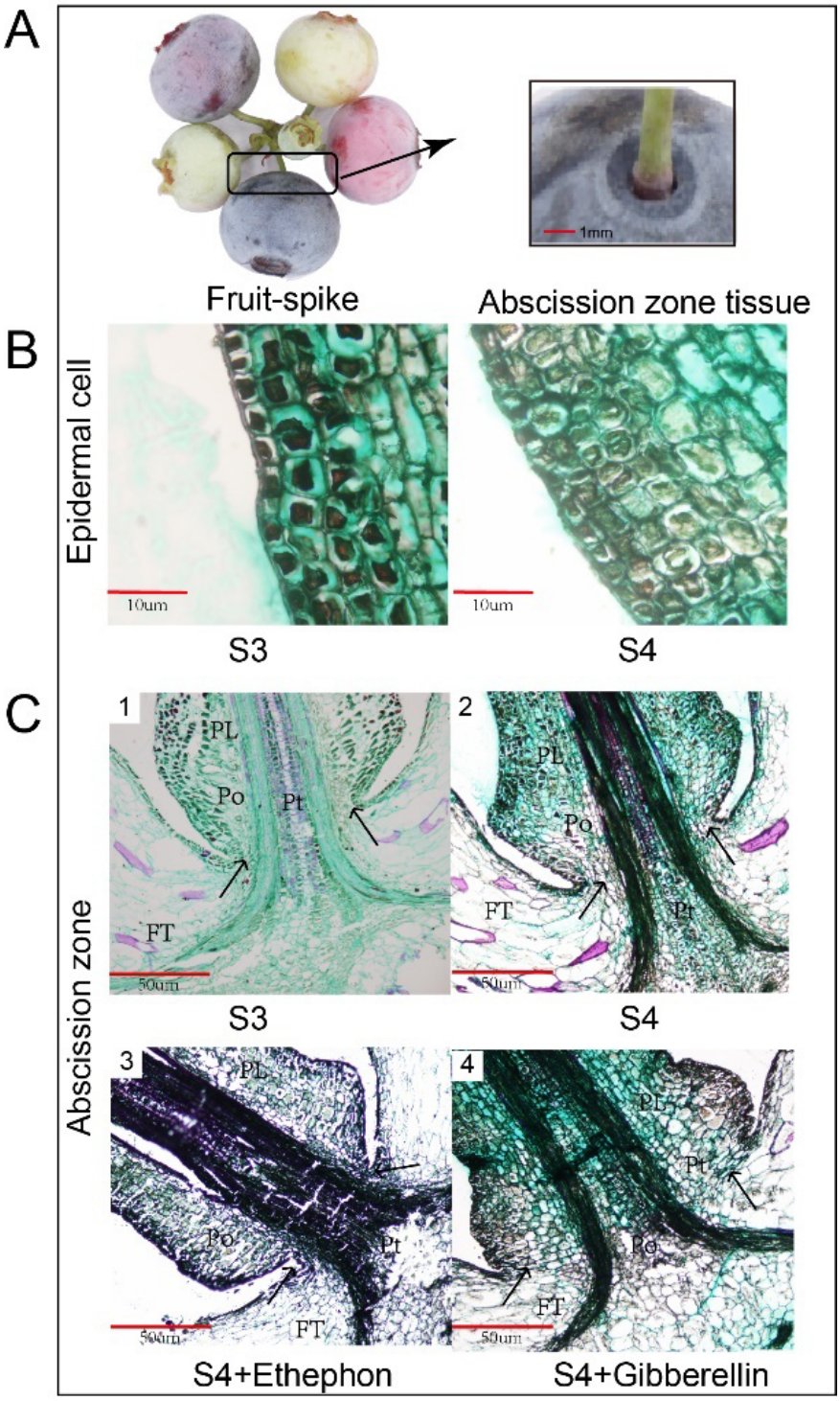

Figure 9

Anatomical and morphological AZs structure of *Vaccinium ashei*. **A** Fruit-spike and abscission zone tissue. The rectangular box refers to the fruit-pedicel junction. **B** Epidermal cells in S3 and S4. **C** Morphological structure of AZ cell layers in veraison (S3) and fully ripe (S4) stage, and those treated with ethephon and gibberellins. Phloem (Po), pith (Pt), pedicel (PL), and fruit (FT).

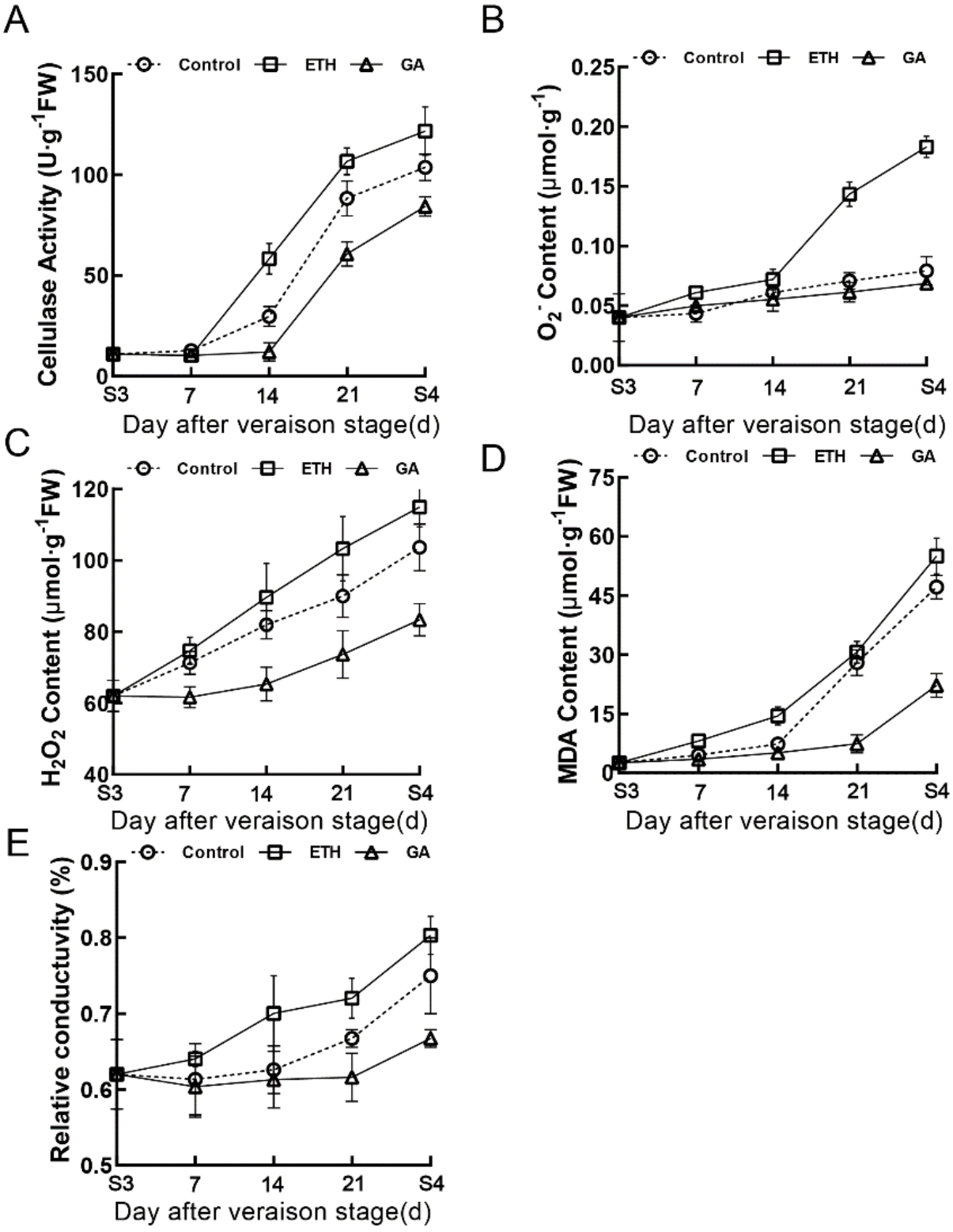

Figure 10

Cellulase activity, and the contents of ROS, MDA, and relative conductivity in fruit AZs of *Vaccinium ashei.* The data represent mean of three replicates with three biological repeats. Error bars indicate SE.

Supplementary Files

This is a list of supplementary files associated with this preprint. Click to download.

- TableS1.xls
- TableS2.xlsx
- TableS3.xls
- TableS4.xls
- TableS5.xls